We are IntechOpen, the world's leading publisher of Open Access books Built by scientists, for scientists

6,900
Open access books available

185,000
International authors and editors

200M
Downloads

Our authors are among the

154
Countries delivered to

TOP 1%
most cited scientists

12.2%
Contributors from top 500 universities



WEB OF SCIENCE™

Selection of our books indexed in the Book Citation Index in Web of Science™ Core Collection (BKCI)

Interested in publishing with us?
Contact book.department@intechopen.com

Numbers displayed above are based on latest data collected.
For more information visit www.intechopen.com



Chapter 4

Forty Years of the d_1/d Parameter

Alexander I. Kokorin

Additional information is available at the end of the chapter

http://dx.doi.org/10.5772/39123

1. Introduction

Spin labeling, as a part of electron paramagnetic resonance (EPR), became one of the most sensitive and adequate methods for investigation the structure, properties of different biological systems, their dynamics, and mechanisms of various processes after opening a new class of chemical reactions of stable nitroxide radicals, in which the unpaired electron remained untouched and retained its paramagnetic properties (Neiman et al., 1962, Rozantsev, 1964, 1970, Rozantzev & Neiman, 1964). Just at once, spin labels, attached to biological (proteins, oligopeptides, polysaccharides, nucleic acids) or synthetic macromolecules, and probes, incorporated into biological or artificial membranes, polymers, solid materials and solutions, have been applied for investigation structural and functional properties of such complex and supra-molecular systems. Harden M. McConnell, O. Hayes Griffith, Gertz I. Likhtenstein, Anatoly L. Buchachenko, Lawrence J. Berliner, Alexander Kalmanson, Geoffrey R. Luckhurst, Jack H. Freed, Andrey N. Kuznetsov, and some others, were first pioneers in this area. Much detailed, the historical aspects of spin label technique are described in chapter written by L. J. Berliner. Great advances have been achieved in practical applications of numerous amount of mono- bi- and poly-radicals synthesized in groups headed by Eduard Rozantsev, John Keana, Andre Rassat, Kalman Hideg, George Sosnovsky, Leonid Volodarsky, Igor Grigor'ev, and their pupils.

First books concerning new method, which are actual up to now, were published approximately in ten years later. Among them, the most cited, are written or edited by Buchachenko & Wasserman, 1973, Likhtenshtein, 1974, Berliner, 1976 & 1979, and Kuznetsov, 1976. Among recent publications, I would like to press attention on several once performing further development and success of this method: Likhtenshtein, 2008, Moebius & Savitsky, 2009, Brustolon & Giamello, 2009, Hemminga & Berliner, 2007, Bender & Berliner, 2006, Schlick, 2006, Webb, 2006. Indeed, high-field (high frequencies) EPR spectroscopy, pulse technique, various double- and multy- resonance methods, time-resolved EPR, etc., enlarged the area of magnetic resonance applications pretty much.

INTECH
open science | open minds

© 2012 Kokorin, licensee InTech. This is an open access chapter distributed under the terms of the Creative Commons Attribution License (http://creativecommons.org/licenses/by/3.0), which permits unrestricted use, distribution, and reproduction in any medium, provided the original work is properly cited.

One of the most important possibilities giving by EPR methods is connected with distance measurements in chemical, biological and nanostructured systems and materials (Parmon et al., 1980, Berliner et al., 2001, Eaton & Eaton, 2004, Steinhoff, 2004, Webb, 2006, Tsvetkov et al., 2008, Moebius & Savitsky 2009), which allows determine distances, two- and three-dimensional distribution of paramagnetic centers, and their mutional orientation in the case of not too long distances.

Stable nitroxide spin probes and labels contain paramagnetic >N–O group with the unpaired electron, surrounding usually with four methyl groups in the appropriate piperidine (R_6, R_6″), pirrolidine (R_5) or imidazoline (R_5^N, R_5^{NO}) rings, which have different "tails" with functional residues in fourth or third positions of the ring, by which probes can be attached to macromolecules, surfaces, etc., becoming spin labels. These radicals are shown in Fig. 1.

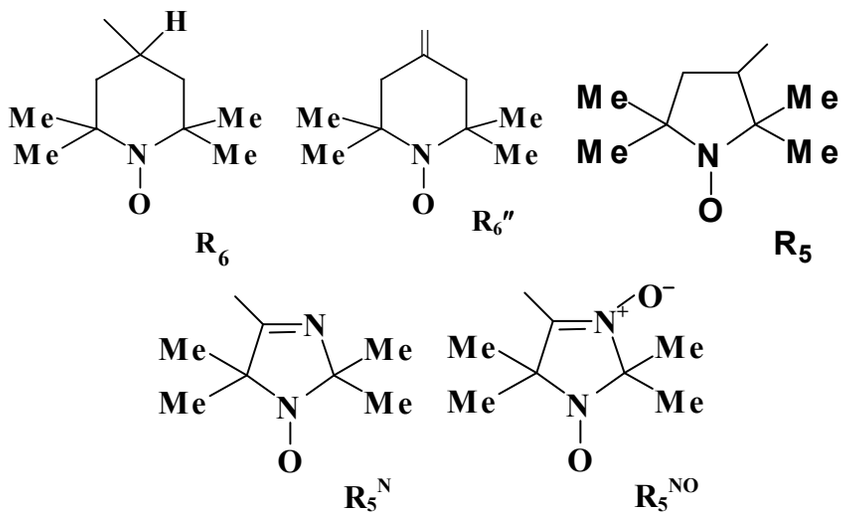


Figure 1. Structures of paramagnetic fragments of nitroxide radicals.

Among spectroscopic methods for determination distances between spin probes, which are discussed in the next section, the simplest one, was developed forty years ago based on empirical parameter d_1/d (Fig. 2) characterizing the shape of the X-band EPR spectrum of the nitroxide radical solution frozen at 77 K (Kokorin et al., 1972). d_1/d is measured with high precision as the ratio of the summed amplitudes of two lateral (low and high field) lines, recorded as the first derivative of the absorption EPR spectrum, to the amplitude of the central component (Fig. 2). It was shown that d_1/d is straightly connected with the efficiency of dipole-dipole coupling between radical paramagnetic >N–O groups, the type of spatial distribution of radicals, as well as with polarity of the surrounding media and temperature of the sample. A methodic procedure of measuring distances is described in detail in Section 3, allows characterize quantitatively the spatial organization of nitroxide biradicals, proteins, nucleic acids, frozen two-component solutions, synthetic polymers, and nanostructured materials. Unfortunately, the most part of the d_1/d features and the majority of the resulta obtained have been published in original only in Russian, though translated into English, scientific journals, and are not known well to practical scientists and students.

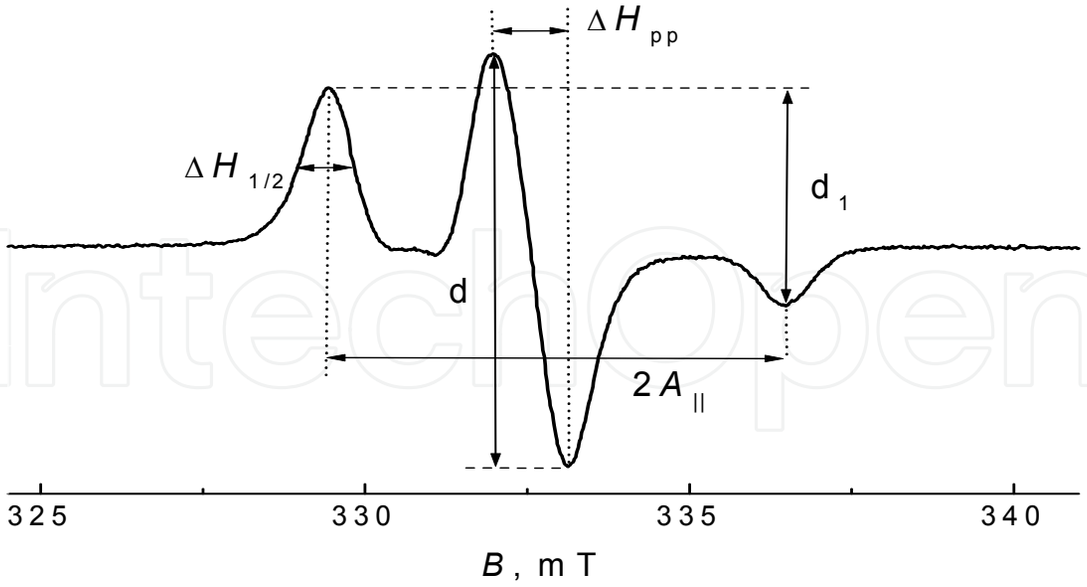


Figure 2. The EPR spectrum of TEMPOL radical at 77 K and c = 0.001 M

Therefore, the main goal of this chapter is describing the present state of this method and the analysis of regularities and peculiarities of its application to various objects and systems under EPR investigation including molecules, macromolecules and supramolecular systems. Theoretical aspects, experimental details, obtained results and conclusions will be reported in the following sections.

2. Methods of the local concentration and the distance measurement from EPR spectra

It is well known from the basic theory of EPR spectroscopy that the value of magnetic dipole-dipole interaction between electron spins of paramagnetic centers depends strongly on the distance between them (Abragam, 1961, Blumenfeld et al., 1962, Altshuler & Kozirev, 1964), and this information is very important for understanding the structure and properties of such systems. There are several independent methods for measuring distances, which have been analyzed in detail in many publications, for example, in the following books: Likhtenshtein, 2008, Moebius & Savitsky, 2009, Berliner et al., 2001, Schweiger & Jeschke, 2001, Eaton & Eaton, 2004, Weil & Bolton, 2007, Tsvetkov et al., 2008, Parmon et al., 1980, Lebedev & Muromtsev, 1971.

The most complete analysis of different approaches and techniques allow measuring distances with high accuracy was presented by Berliner et al., 2001 and Eaton & Eaton, 2004. Below, for better understanding, we shortly report about some of them widely used. Complete information about these approaches one can read in works cited above. It should be mentioned that methods based on double electron-electron resonance, pulsed EPR and spin echo measurements, high frequency and high field EPR are usually used in the case of pairwise interaction between two spins distributed in an immobilized sample (Berliner et

al., 2001). As a rule, a distance between two interacting spins is much less than between different pairs, for example, in the case of nitroxide biradicals in diluted solid solutions or spin labeled proteins.

2.1. Dipolar interaction measured by EPR

Fig. 3 shows typical changes in EPR spectra of R_6OH dissolved in 1-butanol at three different concentrations. Broadening of CW X-band EPR spectra of nitroxide radicals in frozen solutions, due to dipolar interaction, results in changes of the whole spectrum shape which can be characterized with changes in widths of the EPR spectrum lines and in their relative intensities.

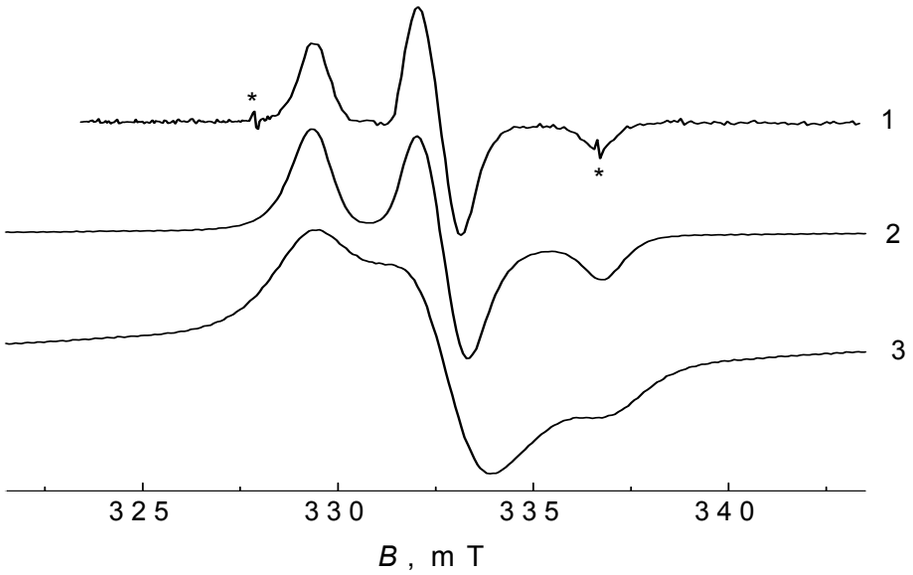


Figure 3. Experimental EPR spectra of R_6OH dissolved in 1-butanol at 0.001 (1), 0.1 (2), and 0.4 mol/l (3) at 77 K. Asterisks * show the 3rd and 4th lines of Mn^{2+} ions in MgO matrix

The line width of the separate line and the shape of whole EPR spectra depend on several various factors such as the distance between paramagnetics, type of their spatial distribution, temperature, polarity, viscosity and organization of the solvent, longitudinal relaxation time T_1, etc. On practice, there are two most common types of distribution: random and pairwise. A quantitative structural characteristic for the first one is the local concertration, C_{loc}. The mean distance among interacting spins, <r>, can be calculated from C_{loc} in an assumption of the distribution type, for the simplest example: $\langle r \rangle = (C_{loc})^{-1/3}$ for cubic regular lattice. For distribution of spins in pairs, for instance, in stable nitroxide biradicals, if they are dissolved at low concentration in solvents glazed under freezing in liquid nitrogen at 77 K, the biradical structure can be completely determined by the certain distance r between two interacting unpaired electrons localized at >N–O bonds, and angles of their mutual spatial orientation (Parmon et al., 1977a, 1980). At high temperatures, if radicals are dissolved in low-viscous liquids with fast rotational and translational mobility, the dipolar coupling is averaged decreasing up to zero.

Dipole-dipole interaction between paramagnetic centers is manifested in dipolar splitting of EPR lines in the case of two coupled spins (biradicals) or in dipolar broadening of EPR lines in the case of interacting of several spins at random distribution. It was shown for the dipolar broadening δH that (Abragam, 1961, Lebedev & Muromtsev, 1971):

$$\delta H = \Delta H - \Delta H_0 = A \bullet C \quad (1)$$

Here ΔH is the width of the homogeneous individual EPR spectrum line, ΔH_0 is a linewidth at the absence of the dipolar coupling, C is concentration, and A is a coefficient, which depends on the character of the spatial distribution of the paramagnetic centres in the sample, the shape of the individual line, and the longitudinal relaxation time T_1. Values of A for different cases of radical distributions (regular, random, in pairs, etc.) are published in (Lebedev & Muromtsev, 1971). For example, the theoretical value $A_{theor} = 5.8 \bullet 10^{-20}$ G/cm^3 = 34.8 G•l/mol for the width at a half-height $\Delta H_{1/2}$ for the Gaussian line shape (Grinberg et al., 1969). Eq.(1) is valid at not too high concentrations, such as $(4/3)\pi r_0^3 C << 1$, where r_0 is the characteristic size of the paramagnetic particle (a distance of the closest approach). Values of r_0 calculated from the experiment were equal to 6.2 ± 0.5 for $R_6OCOC_6H_5$ in toluene, 5.8 ± 0.6, and 6.0 ± 0.4 for R_6OH in ethanol and 50% H_2O-glycerol mixture (Kokorin, 1974).

If the experimental A_{exp} value measured in a wide concentration interval, coincide or close to the A_{theor} value, it is the objective confirmation that paramagnetic species (radicals) are distributed in the whole volume of the sample. In the case of rather often real situation when paramagnetic species are localized in a certain part of the sample only (spin probes in emulsions, in lipid vesicles, spin labels attached to polymer macromolecules, etc.), the experimentally measured value of the parameter $A_{exp} = \delta H/C_{loc}$ characterize the magnitude of the dipolar broadening and can be significantly greater the value of A_{theor}. At the same time, if it is known or can be assumed that for paramagnetic centres used, the type of spatial distribution in the areas of their localization remains the same (random, regular, etc.), the real value of A_{exp} in these areas does not change and has to be equal to A_{theor}. Therefore, one can calculate C_{loc} values by the equation analogues to Eq. (1) (Kokorin, 1992):

$$C_{loc} = \delta H/A \quad (2)$$

Eq. (2) is valid for nitroxide radicals and paramagnetic metal ions with long $T_1 > 10^{-10}$ s (Kokorin, 1992).

It has been experimentally shown that in accordance with Eq. 1, the dipolar broadening of the low-field "parallel" line $\delta H_{1/2}$ and of the central complex line δH_{pp} (see Fig. 2) depends on the radical concentration linearly but with different values of ΔH_0 and A for $\Delta H_{1/2}$ and ΔH_{pp} (Fig. 4).

From these experimental dependences and Eq. 1, one can calculate: A_{pp} = 24.9 ± 0.5 G•l/mol, $\Delta H(0)_{pp}$ = 10.2 ± 0.07 G for all solvents studied; $A_{1/2}$ = 40.6 ± 0.7 G•l/mol, $\Delta H(0)_{1/2}$ is equal to 6.0 ± 0.07, 7.6 ± 0.08, 8.6 ± 0.1 G for R_6OH in frozen at 77 K toluene, ethanol, and 50% glycerol water mixture correspondingly. Very important contribution concerning correct

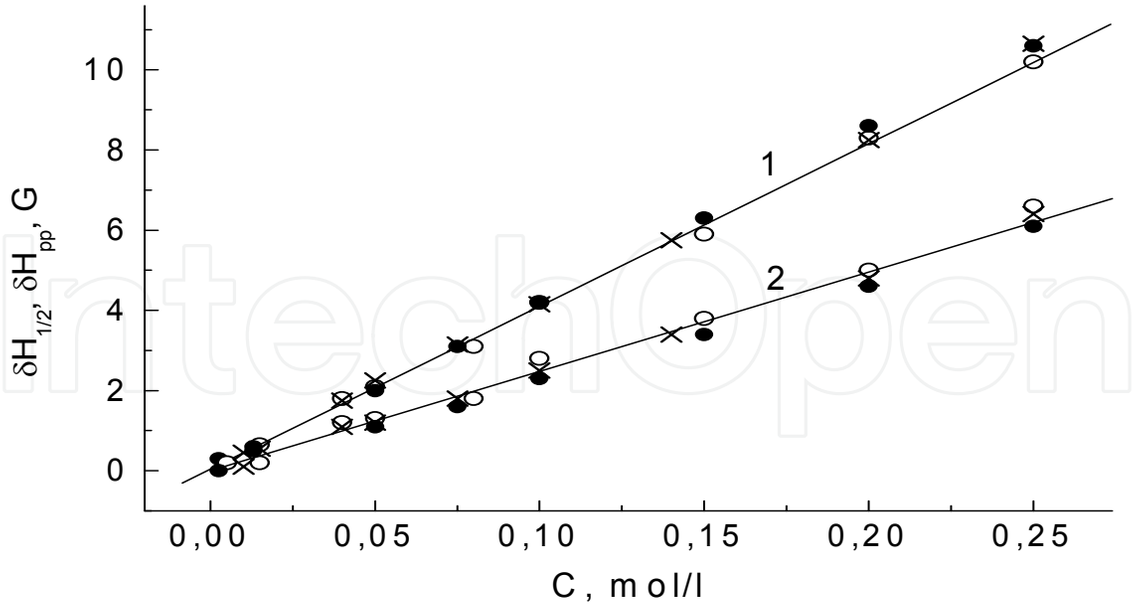


Figure 4. $\delta H_{1/2}$ (1) and δH_{pp} (2) as a function of concentration at 77 K: R_6OH in glycerol:H_2O = 1:1 mixture (○) and in ethanol (×), $R_6OCOC_6H_5$ in toluene (•)

determination of different impacts (dipole-dipole interaction, spin exchange coupling, electron spin relaxation, etc.) to the line broadening of EPR spectra was recently done by Salikhov, 2010.

2.2. Second central moment measured by EPR spectra

Any EPR spectrum can be characterized by its second central moment, which can be determined as:

$$M_2 = \int(H - H_0)^2 F(H)dH / \int F(H)dH, \quad (3)$$

where H_0 is the value of the spectrum centre, F(H) gives the shape of the spectrum absorption line as a function of the magnetic field H, and $\int F(H)dH$ is the normalization condition of the EPR spectrum. The value of H_0 one can find from the equation:

$$\int(H - H_0)F(H)dH = 0 \quad (4)$$

The classical theory of spin-spin interaction connected the value of M_2 with the distance between interacting spins S (Van Vleck, 1948, Pryce & Stevens, 1950):

$$M_2 = (3/4)g^2\beta^2 S(S + 1) \bullet \sum[(1 - 3\cos^2\theta_{j,k})^2 / r_{j,k}^6] \quad (5)$$

Here $r_{j,k}$ is the distance between spins j and k, $\theta_{j,k}$ is the angle between the line connecting these spins and the external magnetic field H, g is a g-factor, and β is Bohr magneton. Later, it was shown by Lebedev, 1969, that the second central moment of the absorption EPR spectrum in the case of the random distribution of paramagnetic centres in a solid matrix depends linearly on their concentration C:

$$M_2 = (2\pi/15)\xi^2 g^2 \beta^2 C_0 C \quad (6)$$

Here $\xi = 3/2$ in the case of the equivalent spins, and $C_0 = r_0^{-3}$ means the characteristic volume occupied by a paramagnetic molecule in the matrix. Hence, linear dependence between M_2 and radical concentration C in solid solutions is evidence of a random distribution of spins in the matrix. Dipole-dipole interaction contributes to the broadening of the spectrum and its second moment M_2:

$$M_2 = M_2(0) + B \bullet C, \quad (7)$$

where $M_2(0)$ is the M_2 value at the absence of dipolar broadening, and a coefficient B is a characteristic of a certain solid matrix, for instance, in magnetically diluted frozen solutions. This dependence is illustrated well in Fig. 5:

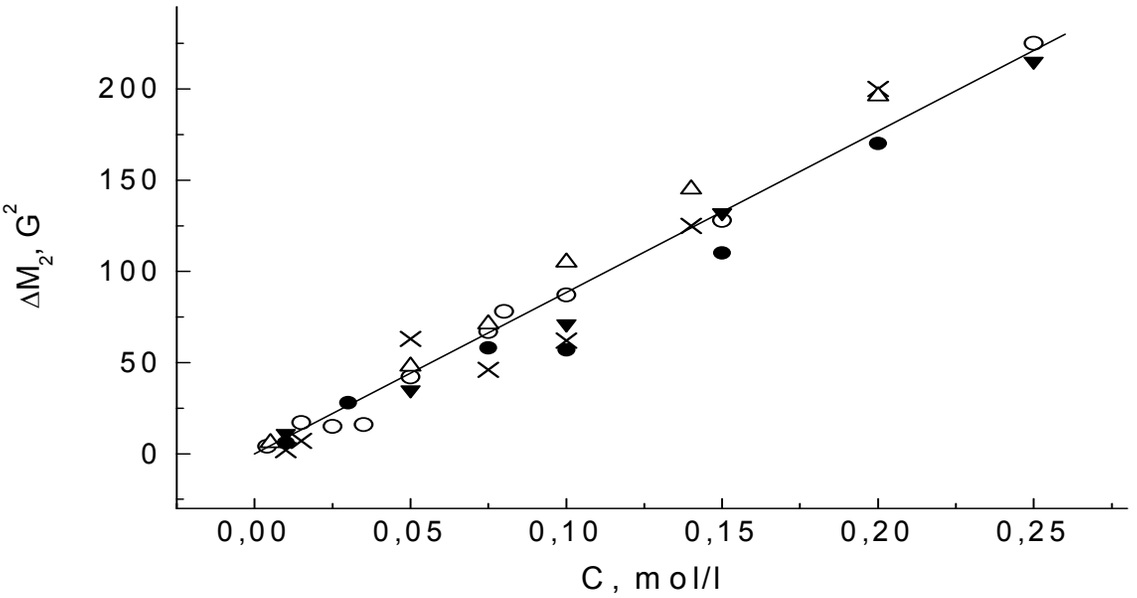


Figure 5. ΔM_2 as a function of concentration at 77 K: R_6OH in glycerol:H_2O = 1:1 mixture (○) and in ethanol (×), $R_6OCOC_6H_5$ in toluene (•), $R_5^NCHCOCH_2I$ in ethanol (Δ), $R_5^NCH_2Br$ in ethanol (▼)

As in the case of dipolar broadening (section 2.1) the local spin concentrations can also be measured from the spectral second central moment M_2 by Eq. (8) in the agreement with Fig. 5:

$$\Delta M_2 = M_2 - M_2(0) = B \bullet C_{loc} \quad (8)$$

The following values were calculated: B = 910 ± 30 G^2•l/mol, and $M_2(0)$ is equal to 340 ± 10, 390 ± 12 G^2 for R_6OH in frozen at 77 K ethanol and 50% glycerol-water mixture correspondingly; 305 ± 6 G^2 for $R_6OCOC_6H_5$ in toluene, 250 ± 10 G^2 for $R_5^NCH_2Br$, and 270 ± 12 G^2 for $R_5^NCHCOCH_2I$ (in ethanol both). $M_2(0)$ is a characteristic of the solvent and the radical structure, while ΔM_2 depends on the magnitude of the dipolar interaction.

Several other useful relations between various spectroscopic parameters are presented in section 3.

2.3. Measurements based on the relaxation time and saturation effects

A method for estimation distances between nitroxide radicals or between spins of the spin label and paramagnetic metal center, based on the quantitative analysis of saturation curves of spin label EPR spectra recorded at 77 K, was suggested by Kulikov & Likhtenstein, 1974. This approach has been tested using haemoglobin molecule labeled by SH groups with various nitroxide radicals. Values of the distances between labels and iron ion in haem estimated from the saturation curve parameters (values of ΔT_1^{-1}, ΔT_2^{-1}, and $\Delta T_1^{-1} \bullet \Delta T_2^{-1}$) were compared with distances measured by d_1/d parameter and estimated from the X-ray data of haemoglobin (Kulikov, 1976). Here, T_1 and T_2 are the longitudinal, T_1, and transverse, T_2, relaxation times of the nitroxide electron spin. Results obtained were in reasonable agreement. In the case of rapid spin relaxation of the metal paramagnetic center, this method allows one determine rather long distances up to 2.0 nm. Serious limitation of this method is the following: for structural investigations of haem containing and other proteins, one have to know the exact value of spin relaxation time T_1 of the metal paramagnetic center from independent measurements (Kulikov, 1976).

Theoretical aspects of the method based on spin relaxation of nitroxide radicals in solid matrix (frozen solutions) were considered in the first part of the review by Kulikov & Likhtenstein 1977. The distance between the spins of the radical and the other paramagnetic centre can be determined from the change of the transverse, T_2, and especially from the longitudinal, T_1, relaxation times of the radical due to the dipole-dipole interaction between the radical and the metal ion. The study of structure of several metal-containing proteins: haemoglobin, myosin and nitrogenase, has been carried out by the method of spin labels. The interesting approach, so called method "spin label – paramagnetic probe" has been carefully examined by spin relaxation in solutions of spin labeled proteins in the presence of inert paramagnetics, readily diffused in the solution by measuring T_2 values of the label. The influence of the probes on labels T_2 values depends on the frequency of collisions between a label and a probe, and therefore this approach can be used for quantitative study of the factors, which effect the frequency of collisions: microviscosity, steric hindrances, the presence of electrostatic charges (Kulikov & Likhtenstein 1977).

Later, many scientists began to work on developing various modifications of the relaxation times method for investigation structural peculiarities and conformational dynamics of biological macromolecules, proteins first of all, their aggregates and bio-membranes. One of the most serious and complete reviews in this field to my opinion was written by Eaton & Eaton, 2001a & 2001b. This review contains theoretical and experimental fundamentals of the method in solid and fluid solutions, technical details, a lot of experimental data, their deep analysis, interesting applications.

2.4. Double electron-electron resonance (ELDOR)

A theoretical basis of the method is perfectly described in (Saxena & Freed, 1997). For calculating double quantum two dimensional electron spin resonance spectra in the rigid

limit, that correspond to the experimental spectra obtained from a nitroxide biradical, a specific formalism has been developed. The theory includes the dipolar interaction between the nitroxide moieties as well as the fully asymmetric g and hyperfine tensors and the angular geometry of the biradical. The effects of arbitrary strong pulses are included by adapting the recently introduced spin-Hamiltonian theory for numerical simulations. Creation of "forbidden" coherence pathways by arbitrary pulses in magnetic resonance, and their role in ELDOR is discussed. The high sensitivity of these ELDOR signals to the strength of the dipolar interaction was demonstrated and rationalized in terms of the orientational selectivity of the "forbidden" pathways. This selectivity also provides constraints on the structural geometry (i.e., the orientations of the nitroxide moieties) of the biradicals. The theory was applied to the double quantum modulation ELDOR experiment on an end-labeled poly-proline peptide biradical. A distance of 1.85 nm between the ends is found for this biradical (Saxena & Freed, 1997).

The results of development of pulse electron-electron double resonance (PELDOR) technique and its applications in structural studies were summarized and described systematically in a review by Tsvetkov et al., 2008. The foundations of the theory of the method were discribed, some experimental features and applications were considered, in particular, determination of the distances between spin labels in the nanometre range for nitroxide biradicals, spin-labeled biological macromolecules, radical-ion pairs, and peptide-membrane complexes. The authors attention was focused on radical systems arising upon self-assembly of nanosized complexes, in particular, from peptides, spatial effects, and radical pairs formation in photolysis and photosynthesis. The position of PELDOR among other structural EPR techniques was analyzed (Tsvetkov et al., 2008).

PELDOR measures via the dipolar electron–electron coupling distances in the nanometre range, currently 1.5–8 nm, with high precision and reliability (Reginsson & Schiemann, 2011). Depending on the quality of the data, the error can be as small as 0.1 nm. Beyond measuring mean distances, PELDOR yields distance distributions, which provide access to conformational distributions and dynamics. The method was also used to count the number of monomers in a complex and allowed determination of the orientations of spin centres with respect to each other. If, in addition to the dipolar through-space coupling, a through-bond exchange coupling mechanism contributes to the overall coupling both mechanisms can be separated and quantified (Reginsson & Schiemann, 2011). This is of principle interest for researchers in many real cases.

Interesting implication of ELDOR to polymer science has been done by Bird et al., 2008.They demonstrated on a series of spin-labeled oligomers quantitative determination the end-to-end lengths and distance distributions. In case of oligomers with well-defined three-dimensional structures (seven different macromolecules, each containing eight monomers) which were labeled with nitroxide radicals, the quantitative information about the shapes and flexibility of the oligomers was obtained, and end-to-end distances were calculared. The shapes of the EPR-derived population distributions allowed authors to compare the flexibility of these spiro-ladder oligomers.

Additional information concerning this very powerful technique one can find in Berliner et al., 2001, Webb, 2006, Reginsson & Schiemann, 2011.

2.5. High frequency/high field EPR spectroscopy

High frequency (high field) EPR spectroscopy opened new approaches for investigating the structure, properties, dynamics, conformational transitions and functioning of many chemical and biological systems. Authors of the recent book considering this method: Möbius & Savitsky, 2009, presented the state-of-the-art capabilities and future perspectives of electron-spin triangulation by high-field/high-frequency dipolar EPR techniques designed for determining the three-dimensional structure of large supra-molecular complexes dissolved in disordered solids. These techniques combine double site-directed spin labeling with orientation-resolving PELDOR spectroscopy. In one of the last publications of this topic, the prospects of angular triangulation, which extends the more familiar distance triangulation was appraise (Savitsky et al., 2011). The three-dimensional structures of two nitroxide biradicals with rather stiff bridging blocks and deuterated nitroxide headgroups have been chosen as a model for spin-labeled proteins. The 95 GHz high-field electron dipolar EPR spectroscopy with the microwave pulse-sequence configurations for PELDOR and relaxation-induced dipolar modulation enhancement (RIDME) has been used. The approach showed good agreement with other structure-determining magnetic-resonance methods, and seems to be one of the most precise orientation-resolving EPR spin triangulation methods for protein structure determination (Savitsky et al., 2011).

To those who want to know about the high field/high frequency approach in detail, I recommend several additional books: Grinberg & Berliner, 2011, Misra, S. K., 2011, Eaton et al., 2010, Hanson & Berliner, 2010.

At the end of this section it is necessary to attract attention to two recent works. The first article considers joint analysis of EPR line shapes and ^{1}H nuclear magnetic relaxation dispersion (NMRD) profiles of DOTA-Gd derivatives by means of the slow motion theory (Kruk et al., 2011). NMRD profiles have been extended to ESR spectral analysis, including in addition g-tensor anisotropy effects. The extended theory has been applied to interpret in a consistent way NMRD profiles and ESR spectra at 95 and 237 GHz for two Gd(III) complexes. The goal was to verify the applicability of the commonly used pseudorotational model of the transient zero field splitting, which was described by a tensor of a constant amplitude, defined in its own principal axes system. The unified interpretation of the EPR and NMRD leads to reasonable agreement with the experimental data. Seems, this approach to the electron spin dynamics can be also effectively used for quantitative description in the case of nitroxide spin probes and labels (Kruk et al., 2011).

One of very important questions in the spin label/probe method is connected with the distance distributions <r> between site-directedly attached spin labels, which obtained by measuring their dipole–dipole interaction in systems under investigation by EPR. As it was shown in (Köhler et al., 2011), the analysis of these distance distributions can be misleading

particularly for broad distributions of <r>, because the most probable distance deviates from the distance between the most probable label positions. The authors studied this effect using numerically generated spin label positions, molecular dynamics simulations, and experimental data of a model systems. An approach involving Rice distributions is proposed to overcome this problem (Köhler et al., 2011).

3. The empirical d_1/d parameter

One of the most informative methods for investigating the structure, spatial organization and physical-chemical properties of complex and supramolecular systems on the microscopic, molecular level is EPR spectroscopy in its spin label/probe technique variant (Berliner, 1976; Buchachenko & Wasserman, 1976; Likhtenstein, 1976). Usually, nitroxide radicals of different structure were used for studying of structural peculiarities of spin labeled proteins and the spatial distribution of probes in them. We will discuss shortly the most important results obtained by different authors below.

With the increase of concentration, X-band EPR spectra of nitroxide radicals in frozen solutions reflect not only dipolar broadening of spectral lines and increasing of the M_2 value, but also noticeable changes of the whole spectrum shape which can be characterized with the empirical "shape parameter" d_1/d (Figs. 2, 3). Anisotropic "frozen" EPR spectra of nitroxide radicals at different widths of individual lines have been simulated (Parmon & Kokorin, 1976). They are shown in Fig. 6.

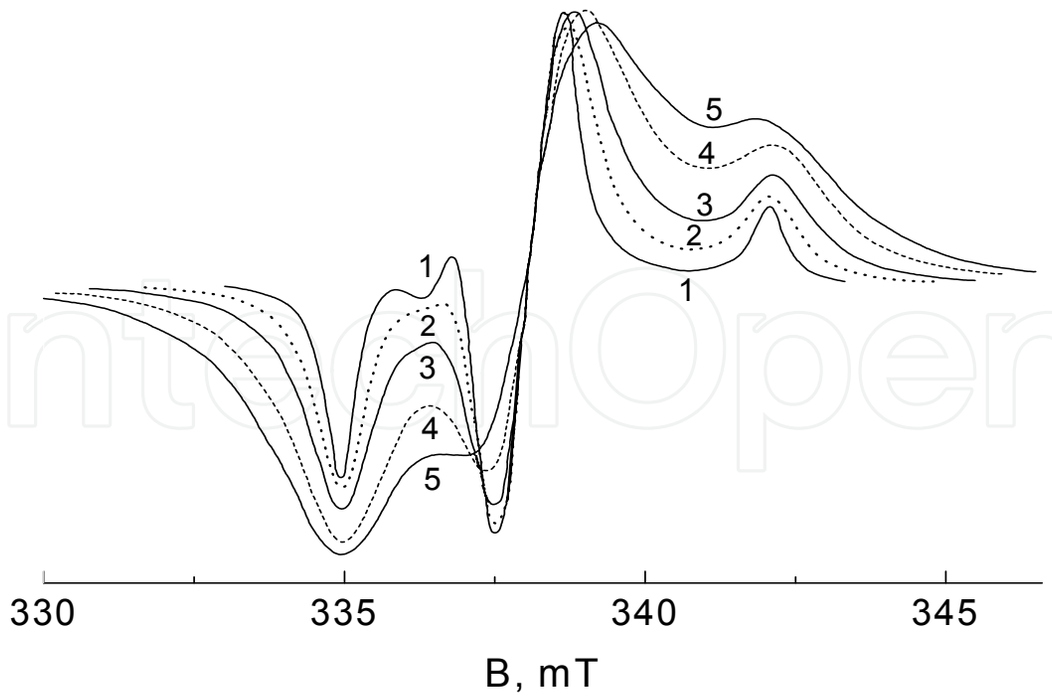


Figure 6. Simulated anisotropic EPR spectra of nitroxide radical at different widths of individual lines: 3 (1), 5 (2), 7 (3), 10 (4), and 13 G (5). The following values were used for simulations: $g_x = 2.0089$, $g_y = 2.0061$, $g_z = 2.0027$; $A_x = 7$, $A_y = 5$, $A_z = 33$ G

It is evidently seen from Figs. 3 and 6 that the line widths and the relative intensities of the center and outer lines in the spectra are changed with the increase of radical concentration. The experimental dependence of d_1/d parameter, characterizing changes of the whole EPR spectrum shape of nitroxides, is not linear (Fig. 7):

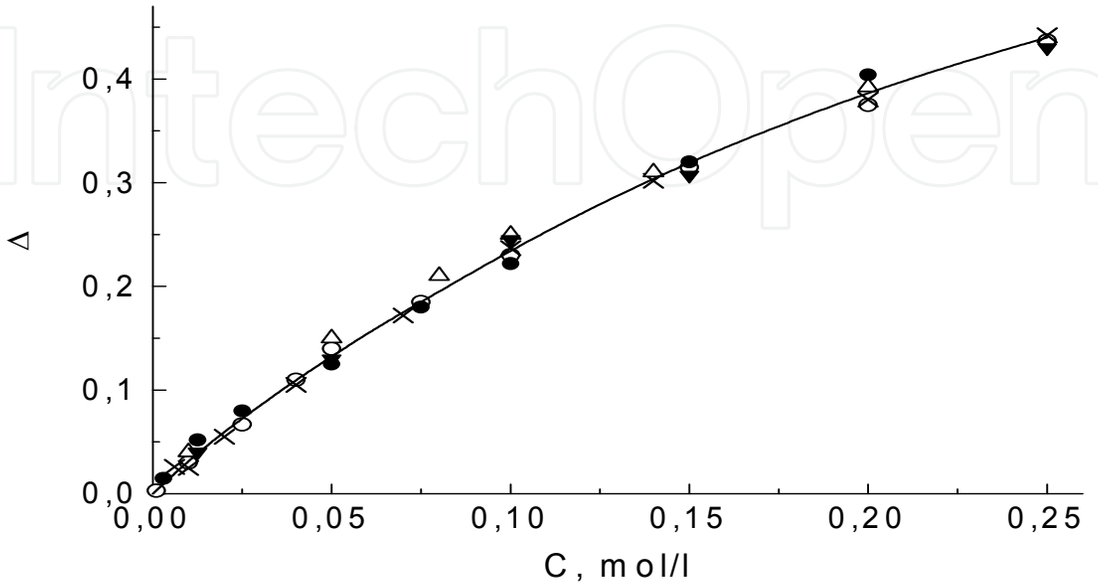


Figure 7. Parameter Δ as a function of nitroxide radical concentration at 77 K: R_6OH in glycerol:H_2O = 1:1 mixture (○) and in ethanol (×), $R_6OCOC_6H_5$ in toluene (•), $R_5{}^NCHCOCH_2I$ in ethanol (Δ) and in toluene (▼)

Similar nonlinear dependence have been obtained from simulations of the anisotropic X-band EPR spectra of nitroxides (Parmon & Kokorin, 1976, Kolbanovsky et al., 1992a). For all nitroxide radicals frozen at 77 K in various glazed solvents studied, one can observe, as it was published by Kokorin et al., 1972, 1975, that:

$$d_1/d = (d_1/d)_0 + \Delta \tag{9}$$

Here Δ is a contribution of the dipole-dipole interaction between radicals, and $(d_1/d)_0$ is a characteristic of the solvent and radical itself (Kokorin, 1974, Kokorin et al., 1975). This equation was verified by precise computer simulations of experimental EPR spectra (Kolbanovsky et al., 1992a). Results obtained for three radicals: R_6OH, $R_6CH_2CH_2Br$ (both in ethanol), and R_6H (in toluene) are given in Table 1. These data confirmed the correctness of usage the d_1/d parameter for quantitative characterization the spatial distribution of spin labels, in the case of their random distribution, in magnetically diluted solid solutions. These results confirmed the possibility of applications of d_1/d parameter for quantitative studies (Kolbanovsky et al., 1992a).

Several experimental correlations between spectral parameters useful for practical applications have been found for nitroxide radicals in solid solutions. They are shown in Figs. 8-10.

C, mol/l	R_6OH		R_6H		$R_6CH_2CH_2Br$	
	Experiment	Theory	Experiment	Theory	Experiment	Theory
0.05	0.12	0.11	0.12	0.12	0.10	0.11
0.1	0.22	0.24	0.23	0.25	0.23	0.23
0.15	0.33	0.37	0.33	0.41	0.31	0.36
0.2	0.38	0.45	0.40	0.49	0.43	0.44
0.25	0.43	0.50	0.43	0.52	0.46	0.48
0.3	0.49	0.54	0.50	0.54	0.51	0.52
0.35	0.55	0.57	0.57	0.56	-	-
0.4	0.58	0.59	0.63	0.57	-	-

Table 1. Experimental and calculated from simulated spectra values of parameter Δ

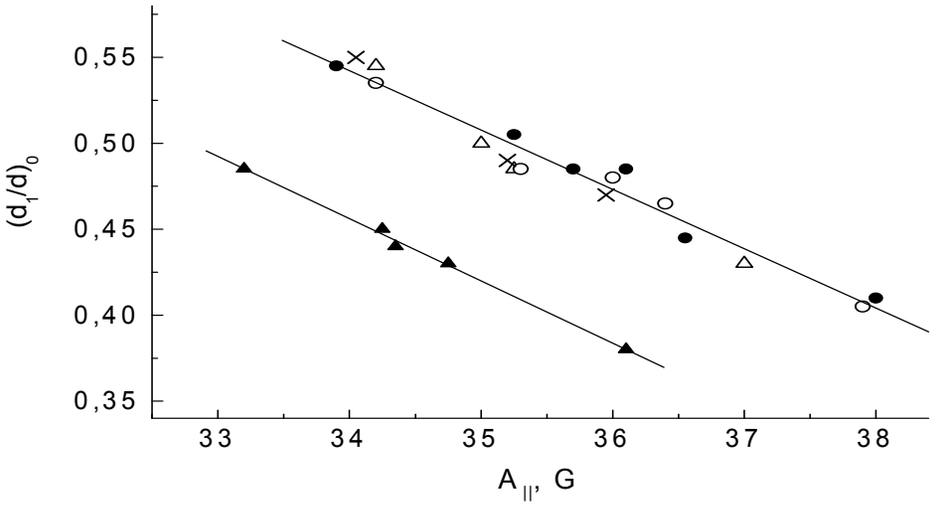


Figure 8. $(d_1/d)_0$ as a function of hyperfine splitting constant $A_{||}$ at 77 K for: R_6=O (▲), R_6H (Δ), R_6OH (○), R_6NH_2 (•), and $R_6OCOC_6H_5$ (×)

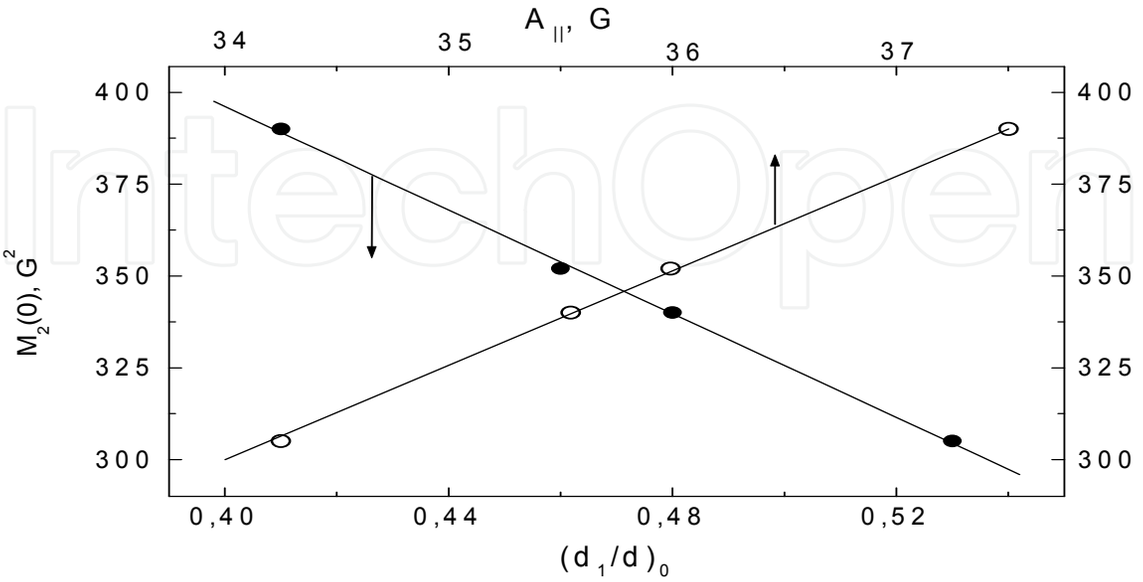


Figure 9. $M_2(0)$ as a function of hyperfine splitting constant $A_{||}$ (○), and of parameter $(d_1/d)_0$ (•) at 77 K for R_6OH in glycerol:H_2O = 1:1 mixture, ethanol, methanol, and $R_6OCOC_6H_5$ in toluene

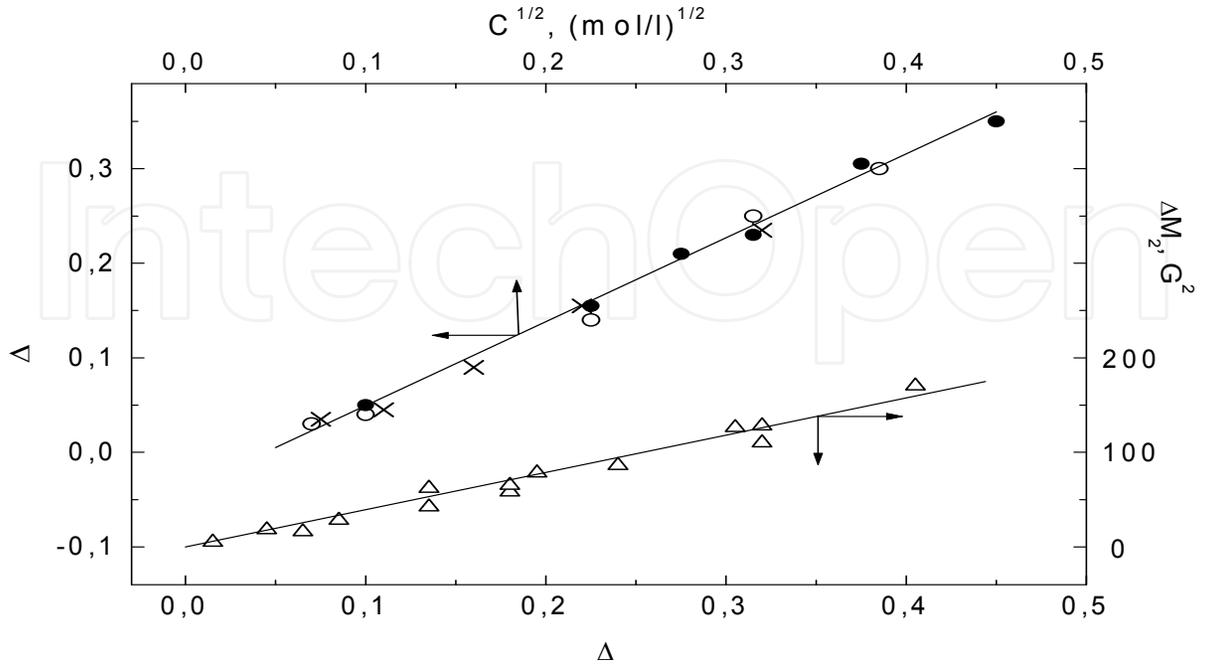


Figure 10. ΔM_2 as a function of parameter Δ (Δ), and parameter Δ as a function of $C^{1/2}$ at 77 K for R_6OH in glycerol:H_2O = 1:1 mixture (×), in ethanol (•), and $R_6OCOC_6H_5$ in toluene (○)

The value of $(d_1/d)_0$ parameter depends on the hyperfine splitting constant $A_{||}$ and on the nitroxide rihg structure (Parmon et al., 1977b). It is seen from Fig. 8 that

$$(d_1/d)_0 = 1.73 - 0.035 \bullet A_{||} \tag{10}$$

These values, 1.73 ± 0.06 and 0.035 ± 0.002, obtained for R_6H, R_6OH, R_6NH_2, and $R_6OCOC_6H_5$ dissolved in various solvents, practically coincide with values of 1.76 and 0.036 correspondingly, published earlier in Parmon et al., 1977b, 1980 and measured for R_6OH radical only. For R_6=O radical, these parameters are equal to 1.70 ± 0.04 and 0.036 ± 0.001, correspondingly.

Fig. 9 presents the value of $M_2(0)$ as a function of $A_{||}$ and of $(d_1/d)_0$ parameter. This can be formalized by corresponding equations:

$$M_2(0) = (25.3 \pm 0.6) \bullet A_{||} - (560 \pm 25) \tag{11}$$

and

$$M_2(0) = (680 \pm 10) - (705 \pm 17) \bullet (d_1/d)_0 \tag{12}$$

Previously (Parmon et al., 1977b, 1980), values of $M_2(0) = 25.5 \bullet A_{||} - 570$ has been reported.

Parameter ΔM_2 also correlates with the values of parameter Δ, as it follows from Fig. 10.

$$\Delta M_2 = (410 \pm 20) \bullet \Delta \tag{13}$$

It was reported (Kokorin, 1986) that parameter Δ, which is not linear on concentration, can be presented as a rather linear plot in other coordinates:

$$\Delta = (0.89 \pm 0.05) \bullet C^{1/2} - (0.025 \pm 0.013) \quad (14)$$

It should be stressed that this linear plot is valid in the concentration range between 0.02 and 0.4 mol/l, i.e., for $0.04 \le \Delta \le 0.45$.

Relations presented above were tested with different objects, and can be recommended for application in the case of random or regular distribution of spin probes in chemical and biological systems.

4. Pairwise interaction between two nitroxide spins

Pairwise distribution of the dipolar interacted spins, when a distance between them, r, is noticeably less than a mean distance between pairs, has been investigated in numerous works. This type of spatial distribution contains first of all nitroxide biradicals and double-labeled proteins, peptides and oligomers. In case of short biradicals with r < 1.1 nm, when the dipolar splitting is observed in the EPR spectrum lines, the r_D value, expressed in Eq. (15), can be easily determined from the spectrum simulation (Parmon et al., 1977a, 1980, Kokorin et al., 1984) or just from the experimental value of the dipolar splitting $D_\perp$ by the equation (Kokorin et al., 1972):

$$r_D = 30.3 \bullet D_\perp^{-1/3}, \quad (15)$$

or from the relative intensity α of the half-field ("forbidden", $\Delta M_S = 2$) and normal-field ($\Delta M_S = 1$) EPR transitions, r_S (Lebedev & Muromtsev, 1972, Dubinskii et al., 1974):

$$\alpha = I_2/I_1 = (8/15)(3g\beta/2H_0\mathbf{r}_S^3)^2 \approx 38/\mathbf{r}_S^6, \quad (16)$$

where I_2 and I_1 are integrated intensities of EPR spectra of corresponding transitions, $H_0 \approx$ 320 mT is a value of the constant magnetic field in the center of $\Delta M_S = 1$ EPR spectrum, and r_S is measured in Å. In practice, the value of rS one can determine experimentally up to 1.2 nm.

The dipolar interaction impact to second central moment $\Delta M_2 = M_2 - M_2(0)$ of EPR spectrum allows measuring the distance r_M (in Å) in biradicals till ~1.8 nm by the equation (Kokorin et al., 1972, Kulikov et al., 1972):

$$\mathbf{r}_M = 23.1 \bullet (\Delta M_2)^{-1/6} \quad (17)$$

Kokorin et al., 1972, reported about 9 biradicals for which distances r were measured independently by methods mentioned above and compared with d_1/d parameter of these biradicals. Later, the number of such "reference" biradicals increased to thirteen, and allowed to plot the experimental dependence of r on Δ presented in Fig. 11 based on the results given in Table 2:

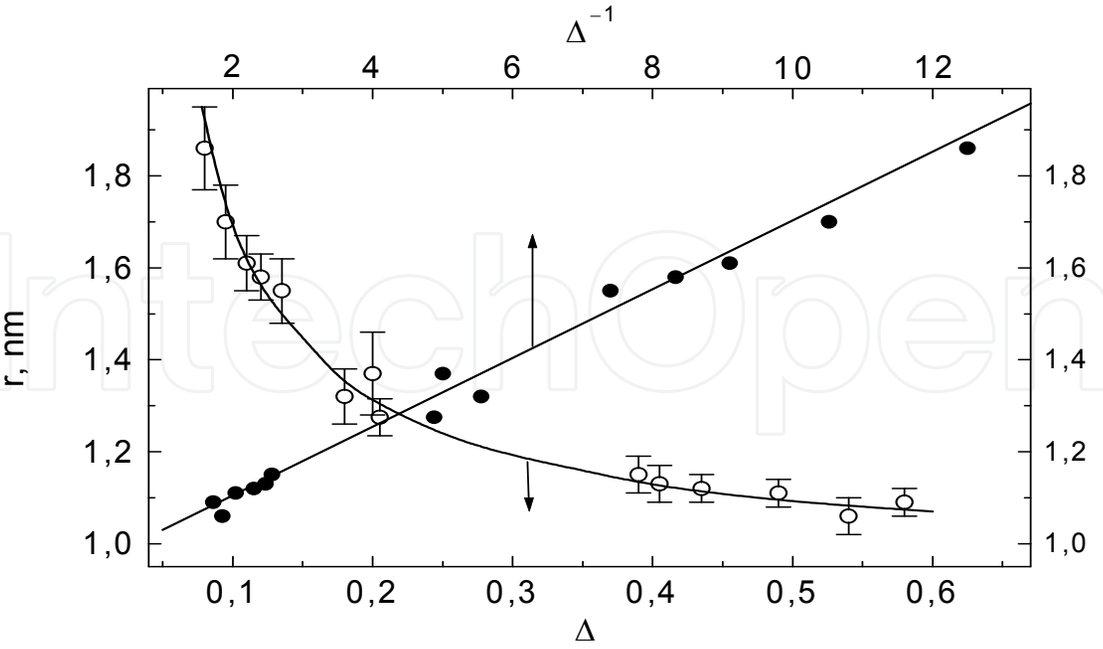


Figure 11. Δ (○) and Δ^{-1} (•) as a function of the distance **r** between unpaired electrons in nitroxide biradicals in frozen solutions at 77 K

Biradical	Solvent	r_M, Å	r_S, Å	r_{calc}, Å
$OC(OR_6)_2$	Toluene	11.2	11.7	11.3*
$S(OR_6)_2$	Toluene	11.1	10.8	11.6
$O_2S(OR_6)_2$	Toluene	10.7	10.3	-
$CH_2CH(O)P(OR_6)_2$	Toluene	10.3	10.2	10.9
$R_6NH(CH_2)_2R_6$	Toluene	10.8	11.5	-
m-$C_6H_4(COOR_6)_2$	Toluene	15.5	-	15.7
o-$C_6H_4(COOR_6)_2$	Toluene	11.5	11.2	11.8
$R_6(CH_2)_4R_6$	Ethanol	12.9	-	13.1*
$(CH_2)_4(HOR_6)_2$	Ethanol	13.6	13.2*	13.8
$(CH_2)_6(COOR_6)_2$	Ethanol	-	18.5*	17.8
m-$N_3C_3Cl^*NHCH_2R_6)_2$	Methanol	13.8	-	13.0
m-$N_3C_3Cl^*NHR_6)_2$	Methanol	11.5	-	11.3

* measured from the X-ray data as the distance between centres of N–O bonds (Capiomont, 1972); r_M measured from the second central moment ΔM_2 (Kokorin et al., 1972, 1974, 1976, Kulikov et al., 1972); r_S measured from the forbidden transitions $\Delta M_S = 2$ (Dubinskii et al., 1974), r_{calc} calculated from EPR spectra simulation at 77 (K (Kokorin et al., 1984)

Table 2. Distances between N–O groups in nitroxide biradicals measured by different methods

Linear dependence of r on Δ^{-1} obtained in the range $1.0 \le \mathbf{r} \le 1.85$ nm gives a correct, simple and rather precise method for the estimation of **r** values: (Kokorin et al., 1976)

$$\mathbf{r} = (9.6 \pm 0.2) + (0.75 \pm 0.02)/\Delta \qquad (18)$$

Kokorin, 1974, Parmon et al., 1977b, 1980 published similar corresponding parameters equal to 9.3 ± 0.25 and 0.77 ± 0.03. One can see that these values are very close to those in Eq. (18). Therefore, the interval in which d_1/d parameter is recommended for correct distance measurements is $1.2 \leq \mathbf{r} \leq 2.5\text{-}2.7$ nm.

Values of <r> and **r** calculated from the EPR spectra simulation for nitroxide radicals and biradicals in the case of random and pairwise distributions according to recommendations of (Kokorin et al., 1984) were compared with experimental data and shown in Fig. 12. Good correlation between experimental and theoretical data is observed.

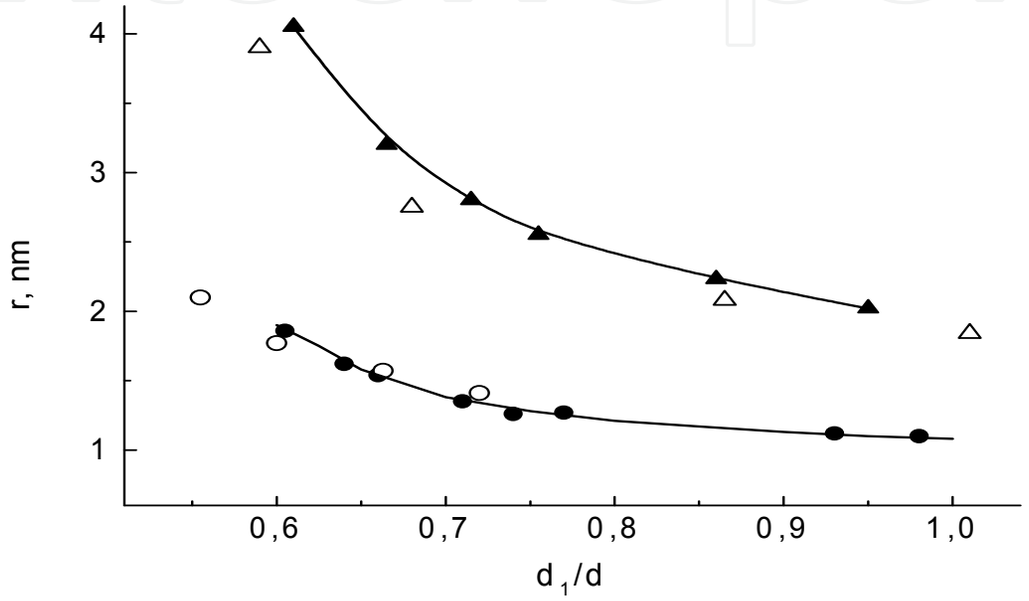


Figure 12. Parameter d_1/d as a function of mean distances <r> for R_6OH radical (Δ, ▲), and distances r for biradicals (○, •) dissolved in frozen at 77 K solutions: experimental (▲, •) and calculated (Δ, ○) from theoretical EPR spectra values

The EPR spectrum shape parameter d_1/d has been used for studying the effect of the solvent on structural organization of nitroxide biradicals.

Results presented in Table 3 show that in glassy solid solutions frozen at 77 K in various solvents the conformational structure of biradicals can be changed by the influence of the solvent in case of non-rigid, rather long flexible molecules such as *m*-$C_6H_4[COO(CH_2)_2R_6]_2$, *o*-$C_6H_4[COO(CH_2)_2R_6]_2$, $S[(CH_2)_2COOR_6]_2$, while for rather short or more rigid molecules ($R_6NH(CH_2)_2R_6$, *m*-$C_6H_4(COOR_6)_2$) the solvent effect is not observed. A long flexible biradical $(CH_2)_4[COO(CH_2)_2R_6]_2$ was not also sensitive to changes in the solvent polarity (Table 3).

It should be stressed that modern EPR techniques allow researchers measuring distances longer 2.5-3.0 nm, which are out of the scale for d_1/d. As an example, it can be illustrated by the work of Bird et al., 2008 in which authors demonstrated the synthesis of a series of spin-labeled curved oligomers and determined their end-to-end lengths and distance distributions using ELDOR technique of EPR spectroscopy. Spin labeled water-soluble, spiro-ladder oligomers with well-defined three-dimensional structures studied with

Biradical	Solvent	$d_1/d \pm 0.01$	r, Å
$R_6NH(CH_2)_2R_6$	Toluene	1.03	11.1 ± 0.2
	Ethanol	0.94	11.0
	H_2O:glycerol = 1:1	0.865	11.0
m-$C_6H_4(COOR_6)_2$	Toluene	0.675	15.5
	1-butanol	0.61	16.0 ± 0.6
	Ethanol	0.60	16.0
	Methanol	0.595	15.7 ± 0.5
o-$C_6H_4[COO(CH_2)_2R_6]_2$	Toluene	0.745	12.7 ± 0.3
	1-butanol	1.01	10.8
	Ethanol	0.92	11.2 ± 0.2
	Methanol	0.82	11.6
m-$C_6H_4[COO(CH_2)_2R_6]_2$	Toluene	0.65	16.1 ± 0.6
	1-butanol	0.55	23.3 ± 2.2
	Ethanol	0.56	19.6 ± 1.4
	Methanol	0.55	19.0 ± 1.2
$(CH_2)_4[COO(CH_2)_2R_6]_2$	Toluene	0.605	20.3 ± 1.6
	Ethanol	0.555	20.3
$S[(CH_2)_2COOR_6]_2$	Toluene	0.66	15.7 ± 0.5
	Ethanol	0.57	18.4 ± 1.0

Table 3. Effect of solvent nature on the distances between unpaired electrons in nitroxide biradicals (Parmon et al., 1980)

ELDOR, provided to obtain quantitative information about the shapes and flexibility of the oligomers. The estimeted end-to-end distance of the oligomers ranges from 23 to 36 Å. The shapes of the EPR-derived population distributions allow the authors to compare the degree of shape persistence and flexibility of spiro-ladder oligomers (Bird et al., 2008).

The last works in this area based on high-frequency pulse EPR technique besides measuring distances allow to determine relative mutual orientation of paramagnetic >N–O groups at distances **r** > 3.0 nm (Savitsky et al., 2011). The 95 GHz high-field electron dipolar EPR spectroscopy with the microwave pulse-sequence configurations for PELDOR has been applied. It was concluded that due to the high detection sensitivity and spectral resolution the combination of site-directed spin labeling with high-field PELDOR stands out as an extremely powerful tool for 3D structure determination of large disordered systems. The authors approach compared with other structure-determining magnetic-resonance methods evidently showed its advantage. Angular constraints were provided in addition to distance constraints obtained for the same sample, and the number of necessary distance constraints was strongly reduced. The reduction of necessary distance constraints became another appealing aspect of orientation-resolving EPR spin triangulation which can be applied for protein structure determination (Savitsky et al., 2011).

Real advantage of d_1/d method in comparison with modern ones is its simplicity, availability and quite good precision within the interval of its correctness (1.2-2.7 nm).

5. Interaction between radicals and paramagnetic metal ions

It was experimentally revealed that d_1/d parameter strongly depends on the longitudinal relaxation time T_1 value, and a new method of measuring distances between spin labels and paramagnetic metal ions in macromolecules suggested (Kokorin & Formazyuk, 1981). The number of paramagnetic metal ions and complexes tested has been enlarged, and possible applications to biological systems discussed (Kokorin, 1986). Some later, this approach has been extended to spin-labeled metal-containing polymers (Kokorin et al., 1989).

Fig. 13 presents typical dependences of d_1/d parameter of R_6OH radical as a function of concentration of R_6OH itself, and of some salts: $Cu(NO_3)_2$, $Ni(en)_2(NO_3)_2$, $CoSO_4$, $MgSO_4$ dissolved in H_2O;glycerol (1:1) mixture, and of $Cr(acac)_3$ in methanol solution. One can see from Fig. 13 that the efficiency of d_1/d increase is different for various metal ions. Indeed, it is known from theory that the dipolar broadening of EPR spectra depends besides concentration of paramagnetic centres on the value of its electron spin and the longitudinal relaxation time T_1 (Abragam, 1961, Molin et al., 1980). Kokorin et al., 1981 suggested to characterize relative efficiency of dipole-dipole interaction between nitroxide radicals and paramagnetic metal ions with parameter α^*:

$$\alpha^* = [4S(S+1)/3]^{-1/2} \bullet <\Delta_M/\Delta_R> \qquad (19)$$

Here Δ_M and Δ_R are the dipolar impacts to d_1/d parameter measured at the same concentrations in cases of interaction between radicals, Δ_R, or between a radical and a metal ion, Δ_M, $<\Delta_M/\Delta_R>$ is the averaging by all concentrations (Fig. 13), and coefficient $\varphi = [4S(S+1)/3]^{-1/2}$ is used for metal ions with the electron spin $S > ½$, and takes into account that a spin probe interacts with several electron spins of the metal, S. In such case the dipolar broadening parameter, A*, will be equal to:

$$A^* = \varphi \bullet \delta H/C_M , \qquad (20)$$

analogous to Eq. (1). This correction allows one to determine local concentrations of various paramagnetic metal complexes. A value of $<\Delta_M/\Delta_R>$ parameter depends on the T_1 value of the paramagnetic centres under investigation (Kokorin & Formazyuk, 1981). Other approaches for solving this problem as well as a perfect collection of experimentally measured values of T_1 are collected in Eaton & Eaton, 2001a, 2001b.

In case of coupling between a nitroxide radical and a paramagnetic metal complex distributed in the matrix in pairs, interesting results were presented by (Fielding et al., 1986). Low-spin Fe(II1)-tetraphenylporphyrin complexes have been modified with seven nitroxide radicals of different length: $-CONHR_{5,6}$, $-CONHCH_2R_{5,6}$, $-OCH_2CONHR_6$, $-O(CH_2)_2CONHR_6$, $-O(CH_2)_4CONHR_6$. The spin labels were attached by amide or amide and ether linkages to the ortho position of one phenyl ring. The axial ligands were imidazole

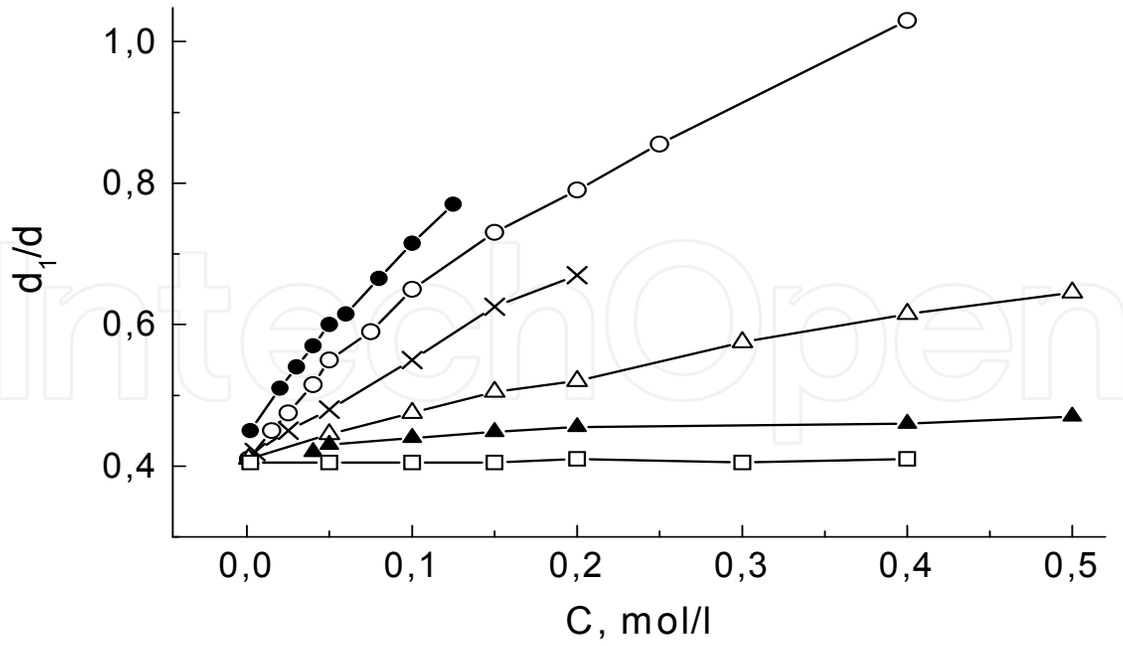


Figure 13. d_1/d as a function of concentration of R_6OH radical (o), $Cu(NO_3)_2$ (×), $Ni(en)_2(NO_3)_2$ (Δ), $CoSO_4$ (▲), $MgSO_4$ (□) in H_2O;glycerol = 1:1, and $Cr(acac)_3$ (●) in methanol at 77 K. en is $NH_2CH_2CH_2NH_2$, and acac is acetylaceronate

or 1-methylimidazole. In frozen solution the complexes with amide linkages adopted two different conformations, and the populations of the conformations were solvent-dependent. Measured value of the exchange integral J was rather high, while the spin-spin interaction in the second conformation was much weaker than in the first conformation. Broadening of the nitroxyl signal in frozen solution was also observed for complexes with longer ether linkages between the phenyl ring and the nitroxyl. Distances between nitroxide N–O groups and Fe(III) ions were estimated by d_1/d parameter and by the Leigh method (Leigh, 1970). The EPR spectra, reported by other authors, of two spin labels coordinated to ferric cytochrome P450 were analyzed with the computer programs developed for the iron porphyrin model systems. The authors showed that electron-electron exchange interaction as well as dipolar interaction must be considered in analyzing the spectra of spin-labeled porphyrin-containing bio-macromolecules (Fielding et al., 1986).

6. Applications to solid solutions and materials

Nitroxide spin probes were successfully used for quantitative investigating the structure and micro-phase organization of frozen two-component solutions (Kokorin & Zamaraev, 1972). R_6OH radical has been chosen as a spin probe to test the homogeneity of heptane-ethanol, carbon tetrachloride-ethanol, and toluene-ethanol mixtures with different ethanol content, frozen at 77 K. EPR spectra of the probe showed non-linear changes of d_1/d parameter, from which local concentrations C_{loc} were calculated. For explanation of the results observed the existence of two different phases in frozen mixed solutions was assumed. By the model suggested in (Khairutdinov & Zamaraev, 1970, Kokorin &

Zamaraev, 1972), radicals were localized not in the whole volume of the sample (V_0, C_0) but only in one mixed phase of total volume V contained both components with local concentration C_{loc}. The second phase was crystallized and did not contain spin probes. Evidently, $C_{loc} = C_0 \bullet V_0/V$ and it was obtained for the coefficient of non-uniformity of probes distribution $\rho = C_{loc}/C_0$:

$$\rho = [(M_{gl}/d_{gl}) + n \bullet (M_{cr}/d_{cr})]^{-1} \bullet C_{Et}^{-1}, \quad (21)$$

where M_{gl}, M_{cr} and d_{gl}, d_{cr} are molecular masses and densities of the glazed (ethanol) and crystallized (heptane, CCL_4) components of the mixture; n is a number of molecules of the crystallized solvent per one molecule of the glazed one (ethanol) in the areas of the spin probe localization. C_{Et} is the concentration of ethanol in the solution. From experimental dependences of ρ on C_{Et}^{-1} for mixtures heptane-ethanol and CCL_4-ethanol a phase of non-polar solvent and the binary mixture of constant composition were observed. The quantitative composition of binary mixtures was determined: 6.5 ± 0.8 ethanol molecules per one heptane molecule, and 2.3 ± 0.3 ethanol molecules per one CCl_4 molecule. Binary toluene-ethanol mixtures were glassy at 77 K at all ratios of components, had complex non-linear dependence of ρ on C_{Et}^{-1} but did not have phases of constant composition (Kokorin & Zamaraev, 1972).

Another interesting and important quantitative application of spin label technique and d_1/d parameter can be illustrated by studies of gold nanoparticles with EPR spectroscopy.

Ionita et al., 2004, investigated the mechanism of a place-exchange reaction of ligand-protected gold nanoparticles using biradical disulfide spin labels which were chemically attached to the surface (Fig. 14). Analysis of reaction mixtures combined GPC and EPR technique allowed authors to determine concentration profile of spin probes and propose a kinetic model for the reaction. Local concentrations of spin labels and mean distances between them were measured using d_1/d parameter. In the model suggested, only one branch of the disulfide ligand was adsorbed on the gold surface during exchange, and the other branch formed mixed disulfide with the outgoing ligand. The two branches of the disulfide ligand therefore did not adsorb in adjacent positions on the surface of gold nanoparticles. This was proven by the powder EPR spectra of frozen exchange reaction mixtures. The data presented also suggested the presence of different binding sites with different reactivity in the exchange reaction. It was assumed that the most-active sites are likely to be nanoparticle surface defects (Ionita et al., 2004).

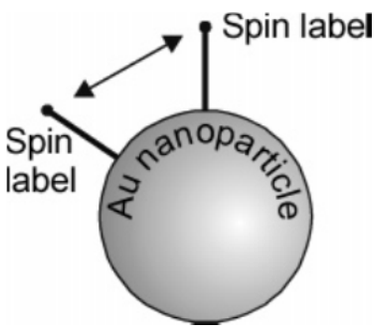


Figure 14. Schematic localization of spin labels on the surface of gold nanoparticles (Ionita et al., 2005)

A series of gold nanoparticles modified with a nitroxide-functionalized ligands was synthesized with a range of spin-label coverage (Ionita et al., 2005). The X-band EPR spectra of frozen solutions of these nanoparticles showed coverage-dependent line-broadening due to dipole-dipole interactions between spin labels, and a noticeable increase of d_1/d parameter. A methodology to analyze such spectra in terms of geometrical features of the nanoparticles (e.g., gold core size and the length of the spin-labeled ligand) was developed. The method was based on the assumption that the spectral line shape was determined by the average distance between nearest-neighboring spin labels adsorbed on the gold particle. Geometrical and statistical analysis related this distance to the line shape parameter d_1/d, which was calibrated using a model system. A calibration curve was suggested as an empirical Eq. (22) (Ionita et al., 2005):

$$d_1/d = a_1 \exp[-a_2(r_n - a_3)] + a_4 + a_5/r_n \quad (22)$$

Here r_n is the average distance between nearest-neighboring nitroxide labels. The values of empirical parameters a_1-a_5 were equal to 0.8050, 3.0150 nm^{-1}, 0.8736 nm, 0.5145, and 0.06824 nm, respectively, as obtained by nonlinear regression. Experimental and calculated values of d_1/d parameter were compared and have been very close to each other. The interspin average distances r_n between nearest-neighboring spins were determined in the range $1.46 \leq r_n \leq 3.3$ nm, and they decreased with increasing coverage of spin labels.

Application of this methodology to the experimental spectra provided information about the conformation of ligands on the gold surface. It was found that, if the spin-labeled ligand was substantially longer than the surrounding protecting layer, it did not adopt a fully stretched conformation but wrapped around the particle immediately above the layer of surrounding ligands. The results obtained also showed that the ligands were not adsorbed cooperatively on the gold surface (Ionita et al., 2005).

The lateral mobility of the thiolate ligands on the surface of gold nanoparticles was also probed by Ionita et al., 2008, using bisnitroxide ligands, which contained a disulfide group in the bridge (to ensure attachment to the gold surface) and a cleavable ester bridge connecting the two spin-labeled branches of the molecule. Upon adsorption of these ligands on the surface of gold particles, the two spin-labeled branches were held next to each other by the ester bridge as evidenced by the spin-spin interactions. Cleavage of the bridge removed the link that kept the branches together. CW and pulsed EPR (ELDOR) experiments showed that the average distance between the adjacent thiolate branches on the gold nanoparticle surface only slightly increased after cleaving the bridge and thermal treatment. This implied that the lateral diffusion of thiolate ligands on the nanoparticle surface was very slow at room temperature and took hours even at elevated temperatures (90°C). The changes in the distance distribution observed at high temperature were likely due to ligands hopping between the nanoparticles rather than diffusing on the particle surface (Ionita et al., 2008).

7. Applications to polymers

Another quantitative application of d_1/d parameter was suggested for determining local concentrations of chain units in macromolecular coils using the spin-label method (Kokorin

et al., 1975). Labelling of poly-4-vinyl-pyridine (P4VP) with $R_6CH_2CH_2Br$, R_6OCOCH_2Cl or $R_6NHCOCH_2I$ radicals with the degree of alkylation of pyridine residues from 2 up to 35 mol.% allowed authors to determine such important structural characteristics of the polymer coil as local concentration of pyridine monomers C_N, the effective volume <V> and effective radius R_{eff} of the polymer coil, its local density ρ_{loc}:

$$<V> = n/C_{loc};\ R_{eff} = (3n/4\pi C_{loc})^{1/3};\ C_N = [(P - n)/n] \bullet C_{loc};\ \rho_{loc} = P \bullet C_{loc}/n \quad (23)$$

Here P and n are a degree of polymerization (mean number of monomer units in the chain) and mean number of spin labels in the coil correspondingly. It should be stressed that this approach is correct if: a) distribution of spin labels in the coil is statistically random, b) the mean volume <V> occupied by spin labels is identical to the volume of the coil, and c) spin labeling does not change the conformation of macromolecules.

High values of C_N equal to 0.3 ± 0.1 mol/l, obtained for labeled P4VP molecules in dilute solutions, confirm the theoretical estimations made by Tanford, 1961. Table 4 contains some values obtained for spin labeled P4VP, polyethylenimine (PEI), polyglycidylmethacrylate (PGMA), poly(methacrylic acid) (PMAc), and its sodium salt (PMAcNa). $<\hat{h}^2> = 6 \bullet (3<V>/4\pi)^{2/3}$ is the mean-square end-to-end distance for a Gaussian chain.

This approach was successfully used for analyzing the conformational state of PGMA macromolecules in diluted and concentrated polymer solutions (Shaulov et al., 1977). Determination of mean distances between monomer units in the chain or their local concentration, C_{loc}, in the effective macromolecular volume <V> as a function of the polymer concentration in solutions of different thermodynamic quality as well as in a solid amorphous powder was carried out. Both labelled and non-labelled polymers were used. It was revealed that within limits of the experimental conditions, the size of the coil considered to be Gaussian, exceeds theta-dimensions, while the coil size in solid polymer is close to θ-dimensions. Models of concentrated PGMA solutions were analyzed and the most probable one was chosen basing on the experiment (Shaulov et al., 1977).

The local density of monomer units of the macromolecule (local density of the host residues, ρ_{host}) in poly(4-vinyl pyridine) solutions in ethanol was determined by the spin label technique and d_1/d parameter (Wasserman et al., 1979). In dilute solutions, ρ_{host} is considerably greater than the mean density of monomer units in the volume of the polymer coil. When the P4VP concentration increases from 0.5 to 65 wt%, the ρ_{host} increase does not exceed 30%. This fact indicates that the differences between polymer coil spatial organization (mutual positions of monomer units close to a labeled unit) in dilute and concentrated solutions are small. The local density of monomer units of neighbouring macromolecule coils (guest macromolecules, ρ_{guest}) is strongly dependent on the polymer concentration in solution. In dilute solutions, $\rho_{host} >> \rho_{guest}$; for polymer concentrations above 2–3 wt%, overlapping and interpenetration of macromolecular coils take place, local density of guest coils, ρ_{guest}; monotonously increases with polymer concentration growing up. The concentration dependence of the local rotational and translational mobility of chain units was also determined for spin-labeled P4VP (Wasserman et al., 1979).

Several works were published in which d_1/d parameter was used for the study of intramolecular dynamics and of local density of P4VP units in diluted and concentrated liquid and frozen solutions with spin label method Wasserman et al., 1980a, 1980b). Temperature dependences of EPR spectra lines of spin labeled P4VP solutions in ethanol allowed estimate dipolar and spin exchange impacts, and to calculate mean local densities ρ_{loc} at 77 and 293 K. Measured parameters: 0.3 ± 0.1 at 77 K and 0.25 ± 0.05 mol/l at 293 K, were several times higher than the average concentrations of the units in solutions. Knowledge of these concentrations allowed to calculate correct diffusion coefficients of spin labels in the P4VP coil. These results are reasonably close to those listed in Table 4.

Polymer	P	C_{loc}, mol/l	ρ, mol/l	$\langle V \rangle$, nm^3	R_{eff}, nm	$\langle \hat{h}^2 \rangle$, nm^2
P4VP-25%	430	0.14	0.52	1370	6.8	280
P4VP-35%	270	0.17	0.49	930	6.1	220
P4VP-10%	1330	0.04	0.4	5540	11.0	726
P4VP-15%	1330	0.07	0.49	4570	10.3	636
P4VP-20%	1330	0.11	0.55	4030	9.9	590
P4VP-28%	1330	0.14	0.5	4430	10.2	624
P4VP-40%	1330	0.18	0.45	4930	10.6	670
PEI-5%	120	0.023	0.46	435	4.7	130
PEI-22%	120	0.14	0.62	320	4.25	110
PGMA-10%	690	0.033	0.33	3450	9.4	530
PGMA-16%	690	0.05	0.3	3830	9.7	560
PMAc-23%	1600	0.11	0.48	5580	9.3	520
PMAcNa-23%	1600	0.1	0.43	6130	9.6	550

Table 4. Some parameters characterizing spin-labelled polymers (Kokorin, 1992, Wasserman et al., 1992)

The intramolecular mobility and local density of monomer units in spin labeled styrene co-polymers with maleic anhydride has been studied (Aleksandrova et al, 1986). The estimated value of ρ_{loc} for these co-polymers dissolved in dimethylformamide equal ≈0.03 mol/l was ten-fold less ρ_{loc} values measured for P4VP in ethanol or 50% H_2O:ethanol mixtures (Table 4).

Quantitative measurements of non-crystallized (solvated) water molecules, based on the EPR study of the structure of frozen aqueous solutions of polyvinylpyrrolidone (PVP) and of polyvinylalcohol (PVA) have been reported (Mikhalev et al., 1985). Local concentrations of spin labels and spin probes were determined by d_1/d parameter and C_{loc} values calculated using procedure suggested in Khairutdinov & Zamaraev, 1970, Kokorin & Zamaraev, 1972. In the presence of NaCl salt in frozen solutions of PVP, the formation of strong complexes between PVP links with water has been observed in the areas containing salt, polymer fragments and H_2O molecules.

The application of EPR spin probe and spin label technique for solving two actual problems of polymer physical chemistry was considered in (Wasserman et al., *1996*). The first problem is the determination of conformational state and chain sizes in amorphous solid polymers.

This determination is based on the analysis of the intramolecular dipolar broadening of EPR spectra of spin labelled macromolecules in glassy solvents or in the bulk of unlabeled polymers at 77 K with the use of d_1/d parameter. The second problem is the determination of molecular dynamics and structure of polymer colloid systems: (a) the complex of colloidal silica and synthetic polycation macromolecule, and (b) polymer-surfactant micellar organized systems. Possible approaches were discussed.

Spin labeling was used to investigate the topochemical characteristics of polymer carriers and immobilized metal complexes (Bravaya & Pomogailo, 2000). Functionalized polyethylene (PE) molecules such as PE-grafted-polyallylamine (PE-PAA), PE-grafted-polydiallylamine (PE-PDAA), and PE-grafted-poly-4-vinylpyridine (PE-P4VP), obtained by grafting polymerization of the corresponding monomers, were used as polymer carriers. Metal-containing polymers were synthesized by attaching to polymers either $TiCl_4$ (PE-PDAA-Ti) or $Al(C_2H_5)_2Cl$ (PE-PDAA-Al). 2,2,6,6-tetramethyl-4-(2'-oxy-4',6'-dichlorotriazine) piperidine-1-oxyl nitroxyl radical (R_1) was used for spin labeling PE-PDAA, while 2,2,5,5,tetramethyl-3-(N-acetoamidiiodine)pyrrollidine-1-oxyl (R_2) was used for spin labeling PE-P4VP, and 2,2,6,6-tetramethyl-4-hydroxy-pyperidine-1-oxyl (R_3) was bound to PE-PDAA-Ti and PE-PDAA-Al respectively. Estimation of the effective distances between the spin labels by d_1/d parameter and the dynamic behavior of nitroxyl radicals in the functionalized polymer matrixes and metal-containing polymers revealed several important features of spin-labeled systems. Metal complex formation of functional polymers made them more accessible for spin labeling and had a considerable effect on the dynamic characteristics of the polymer matrix. Thermodynamic characteristics of the rotational diffusion of the labels were determined (Bravaya & Pomogailo, 2000).

Next serious approach to better understanding structural organization of spin labeled macromolecules in the amorphous solid state and their conformational transitions has been suggested by Khazanovich et al., 1992. The algorithm for EPR spectra computation was developed: it was assumed that molecular weights of labelled linear chains are high enough and their solid solution is diluted. It was shown that the scaling exponent which determines the dependence of mean-square end-to-end distance on molecular weight and stiffness parameter (mean-square length of monomer unit) may be extracted from the spectra. Simulated EPR spectra were compared with experimental ones, measured at 77 K, of diluted solutions of spin-labelled poly(4-vinyl pyridine), P4VP, of different molecular weights in methanol and non-labelled P4VP. The conformational state of the Gaussian coil, parameter of stiffness, and mean square radius of gyration $\langle R_G^2 \rangle^{1/2}$ of spin-labeled P4VP macromolecule in frozen solutions were determined via measuring d_1/d parameter, local density values ρ_{loc} of links, and parameters mentioned above were calculated from it. It was concluded that EPR spectroscopy may become a sensitive tool for studying chain conformation in solid polymers (Khazanovich et al., 1992, Kolbanovsky et al., 1992b).

This approach was successfully used to determine the conformational states of spin labeled P4VP, poly(methacrylic acid), PMAc, and its sodium salt in glassy methanol, ethanol, 1-propanol solutions and in the bulk matrix of unlabeled polymers at 77 K. All macromolecules had near-Gaussian coil conformations. The mean square lengths of the

repeating units, the characteristic ratios, and the mean-square end-to-end distances $\langle R^2 \rangle^{1/2}$ of the polymers were determined. Typical results are listed in Table 5 with corresponding values of Δ (extracted from Wasserman et al., 1992).

Polymer*	Solvent	Δ	$\langle R^2 \rangle^{1/2}$, nm
P4VP-1	Methanol	0.24	22
P4VP-1	1-Propanol	0.29	20
P4VP-2	Methanol	0.14	22
P4VP-4	Ethanol	0.28	36
P4VP-5	Ethanol	0.17	33
P4VP-6	Methanol	0.13	107
PMAc	Methanol	0.25	44
PMAcNa	Methanol	0.23	48

* P4VP-1,2,6 were labeled with $R_6CH_2CH_2Br$, P4VP-4,5 – with $R_5N{=}CHCOCH_2I$, PMAc – with R_6NH_2. P4VP-1,2, P4VP-4,5 and P4VP-6 are of different molecular mass.

Table 5. Parameters Δ and $\langle R^2 \rangle^{1/2}$ of spin labeled macromolecules

Analyzing developing of the area of spin probes and labels during a quarter of a century of its application to polymer studies, the author described in details history of the method, investigations of local and segmental mobility in polymers, and paid special attention to the approaches for determining local densities and translational dynamics of monomeric units in a coil (Kovarski, 1996).

It should be noted that EPR data on conformational state and dimensions of the polymer coil can substantially complement the data of other physical methods: neutron scattering, for example.

The spin label method was also used for studying the spatial organization of the labeled linear polyethyleneimine (PEI) macromolecules in glassy 50% water-ethanol solutions in the process of complex formation with transition metal ions (Kokorin et al., 1989). The mean local density of PEI chain units ρ_{loc} was measured by d_1/d parameter, as well as PEI coil volume $\langle V \rangle$, the mean coil radius R_{eff}, and the average distance berween spin labels (Table 5). It is known, that if in the sample there are paramagnetic centres of different nature, total dipolar broadening of EPR spectrum lines is the sum of broadenings caused by paramagnetics of each type (Lebedev & Muromtsev, 1972). Analogously, in case of coordination of metal ions (paramagnetic Cu(II), Ni(II), Co(II) and diamagnetic Zn(II) and sodium ions) by the spin-labeled PEI, a procedure for separate determination the impacts of the dipole-dipole interaction between spins of radical labels Δ_{LL} and of radicals with metal ions Δ_{LM} was suggested. These impacts can be expressed as a sum to the experimentally measured value of parameter Δ:

$$\Delta = \Delta_{LL} + \Delta_{LM} \tag{24}$$

The average distances R_{LM} between a label and the nearest paramagnetic complex were determined by the method suggested by Leigh, 1970. The average local concentrations of

complexes <C_M> in the PEI coil volume were calculated using the data and coefficients obtained in Kokorin & Formazyuk, 1981. Changes in Δ_{LL} caused by the decrease of the coil volume as a result of polymer-metal complex formation was determined by measuring d_1/d values in the case of PEI interaction with diamagnetic Zn(II) ions in the whole range of [M]/[L] ratios. As an example of this approach Fig. 15 shows the effective local concentration of metal complexes <C_M> in the PEI coil vs. the metal-to-label ratio [M]/[L] for different metal ions at 77 K (Kokorin et al., 1989).

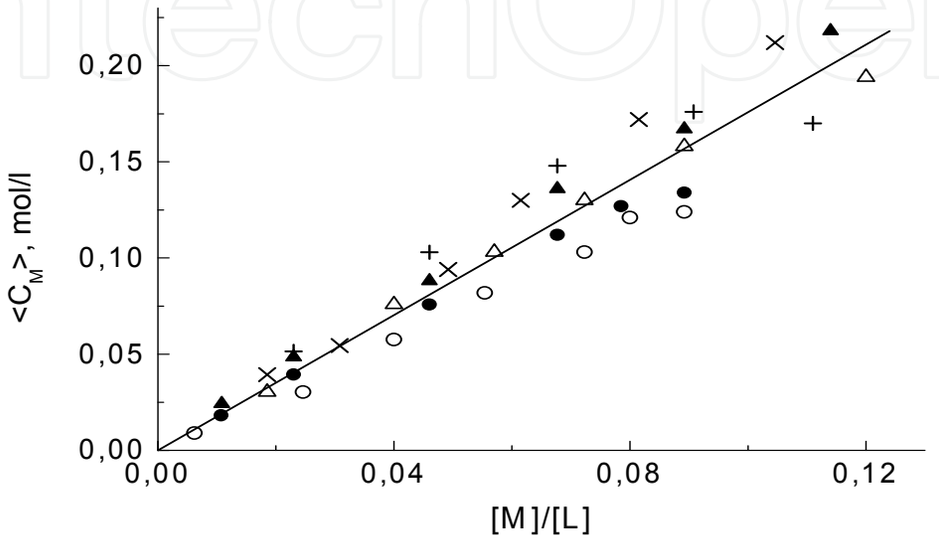


Figure 15. Effective local concentration of metal complexes <C_M> in PEI coil as a function of metal-to-label ratio [M]/[L] at 77 K for: ●,o - Cu(II), ▲,Δ - Ni(II) and ×,+ - Co(II). Concentration of spin labels [L] = 0.045 (●,▲,×) and 0.012 mol/l (o,Δ,+)

It should be stressed that this procedure is correct only in the assumption that spatial distributions of spin labels and polymer-metal complexes in the coil are the same, random, and there are no areas of their specific localization. A fact that <C_M> plots vs. [M]/[L] ratio are the same for all divalent ions studied allows conclude that the structure of metal-PEI coil for these ions is similar.

Determination of the nanostructure of polymer materials by EPR spectroscopy was considered as one of the few methods that can characterize structural features in the range between 1 and 5 nm in systems that lack long-range order (Jeschke, 2002). Approaches based on various techniques of EPR spectroscopy, such as CW X-band EPR, electron spin echo, ENDOR) provided good structural contrast even in complex materials, because the sites of interest could be selectively labeled or addressed by suitably functionalized spin probes using well established techniques. In the article, experiments on distance measurements on nanoscales in terms of the accessible distance range, precision, and sensitivity were discussed, and recommendations were derived for the proper choice of experiment. Both simple and sophisticated methods for data analysis are described and their limitations are evaluated. The approach of Khazanovich et al., 1992, based on d_1/d and Δ parameters was used for characterization of the chain conformation was described. The conformational

organization of the polymer chain and the structure of ionomers based on diblock copolymers were analyzed (Jeschke, 2002).

Bird et al., 2008, demonstrated modern possibilities of ELDOR and computing methods on a series of spin-labeled oligomers to determine their end-to-end lengths, R_{ee}, and distance distributions. Seven different shape-persistent macromolecules from conformationally restricted, asymmetric monomers that are coupled through pairs of amide bonds to create water-soluble, spiro-ladder oligomers with well-defined three-dimensional structures were synthesized and investigated. The ends of these oligomers were labeled with nitroxide radicals. ELDOR experiments were carried out to obtain quantitative information about the shapes and flexibility of the oligomers. The most probable R_{ee} distance of the oligomers ranges from 2.3 to 3.6 nm. The relative distances measured for the oligomers confirm that, by varying the sequence of an oligomer, one can control its shape. The shapes of the EPR-derived population distributions allowed the authors to compare the degree of shape persistence and flexibility of spiro-ladder oligomers to other well-studied nanoscale molecular structures such as *p*-phenylethynylenes (Bird et al., 2008).

Interesting application of spin label method and d_1/d parameter was presented by Kozlov et al., 1981, for investigation the oligomers in solutions where long-chain flexible nitroxide biradicals were used as a model. Measuring distances **r** between N–O groups in oligomers, the dependence of **r** on the number of units in the chain, n, was experimentally obtained for 12 biradicals of different length, and the equation (Flory, 1969):

$$\langle r^2 \rangle = \alpha^2 \beta^2 n, \tag{25}$$

where α is a Flory-Fox constant, and β is the characteristic length. It was shown that $\alpha\beta$ = 0.56 nm for hydrocarbon oligomers, $\alpha\beta$ = 0.534 nm for dimethylsiloxane ones, and also β = 0.452 and 0.405 nm for poly(methylene) and poly(dimethylsiloxane) chains correspondingly (Kozlov et al., 1981). Fig. 16 Illustrates Eq. () well.

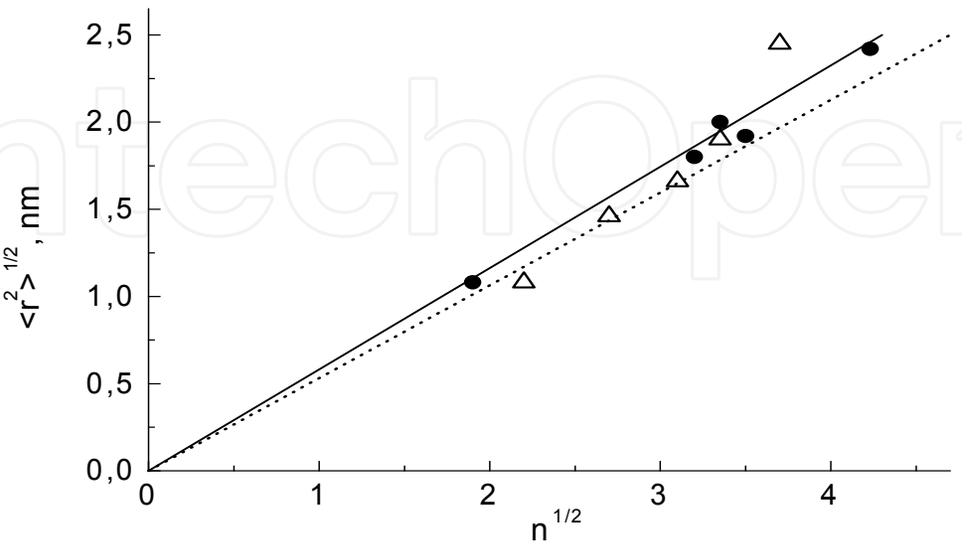


Figure 16. Distance $\langle r^2 \rangle^{1/2}$ as a function of $n^{1/2}$ in toluene solutions at 77 K for $(CH_2)_k(COOR_6)_2$, k = 6-8, 10, 14 (●), and $R_6O–[Si(CH_3)_2O]_m–R_6$, m = 2-6 (Δ)

Additional information on applications of spin label technique for investigation structural properties of synthetic polymers is described in detail in monographs by Wasserman & Kovarsky, 1986, Kovarski, 1996, Schlick, 2006.

8. Applications to biological systems

If two nitroxide spin labels are attached to any biological macromolecule, one can measure a distance **r** between their unpaired electrons from the magnitude of dipole-dipole interaction. This approach has been suggested for the first time by Kokorin et al., 1972, Kulikov et al., 1972. Oxy- and met- forms of spin labelled human haemoglobin (Kokorin et al., 1972), egg lysocyme, cachalot myoglobin and myosin from rabbit muscles (Kulikov et al., 1972) were used as probing macromolecules because at that time the X-ray analysis of these proteins was already done and their spatial organization was known. This provided important possibility to compare EPR results with known X-ray structure. The results obtained in these works demonstrated that measuring the second central moment of EPR spectra one can determine distances r with high accuracy in the range of $1.0 < \mathbf{r} < 1.6$ nm, while the experimental EPR spectrum shape parameter d_1/d shifted the upper value of **r** up to 2.5 nm, what is very important for biological systems. Then, the following equation

$$\mathbf{r} = 9.3 + 0.77/\Delta \tag{26}$$

analogoues to Eq. (18) was suggested (Kokorin, 1974, Parmon et al., 1977b, 1980) for experimental applications. Very often researchers plotted their own graduation curves for using d_1/d parameter. Below, the most interesting results obtained with this parameter in different biological systems are discussed.

8.1. Peptides, proteins, enzymes

The first object to which the approach and d_1/d parameter was applied was D-glyceraldehyde-3-phosphate Dehydrogenase (Elek, et al., 1972), for which authors showed that the distance between spin labels attached to Cys-149 and Cys-153 does not exceed 2.1 nm.

Several works were done on double spin-labelled short proteins – biologically active polypeptides such as Gramicidine S, Bradykinin, etc.

Conformational states of cyclic decapeptide Gramicidine S was studied in (Ivanov et al., 1973). Two ornithine amino acid groups were labeled and at temperatures higher 40°C EPR spectra showed five-component spectra typical for nitroxide biradicals. In frozen solutions the distance **r** equal to 1.25 ± 0.08 and ~1.0 nm was estimated from d_1/d parameter and ΔM_2 value correspondingly, while theoretical calculations of Gramicidine S model estimated the appropriate distance in the range of 1.2 – 1.4 nm.

The most detailed and consecutive study of spatial structure of linear polypeptide Bradykinin was carried out in (Ivanov et al., 1975a, 1975b, Filatova et al., 1977). Attaching by two radicals $R_6CH_2COO–$ or $R_5COO–$ to different amino acid groups as it is shown schematically in Fig. 17:

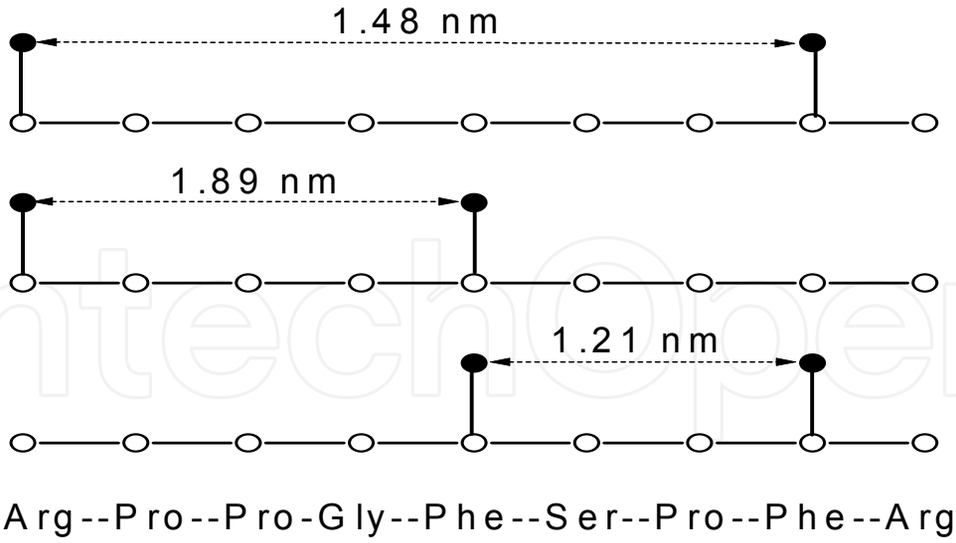


Figure 17. A schematic structure of double spin labelled bradykinin derivatives

The authors could measure a set of distances between various bradykinin analogues. Nine different "biradical" derivatives were synthesized. Some results (parameters d_1/d and **r**) extracted from articles by Ivanov et al., 1975a, 1975b, Filatova et al., 1977, are given in Table 6.

Compound *	d_1/d	r, nm
R_1-Arg^1–Ser^6-R_1	0.64	1.36
R_2-Arg^1–Ser^6-R_2	0.72	1.17
R_1-Arg^1–Tyr^5-R_1	0.57	1.63
R_1-Arg^1–Tyr^8-R_1	0.60	1.48
R_1-Pro^2–Tyr^5-R_1	0.54	1.89
R_1-Pro^2–Tyr^8-R_1	0.58	1.57
BOC-Arg-(R_1)Tyr^5–Tyr^8-R_1	0.65	1.34
BOC-Pro-(R_1)Tyr^5–Tyr^8-R_1	0.56	1.70
BOC-Gly-(R_1)Tyr^5–Tyr^8-R_1	0.65	1.34

* R_1 – R_6CH_2COO–, R_2 – R_5COO–, BOC – *tert*-butyloxycarbonyl

Table 6. Values of d_1/d and interspin distances r in double spin labeled bradykinin derivatives

An important result followed from these data: the bradykinin structure in a solution could not be lenear or chaotically disordered, and the most probable structure was chosen, later confirmed by quantum chemical calculations. It was shown that bradykinin has in solutions a curved, quasi-cyclic structure, which was confirmed by the decay of fluorescence in the case of fluorescent labels.

Study of the interaction between natural and spin labeled steroid hormones and human serum albumin was carried out (Sergeev et al., 1974). The main goal of the work was determination of the relative location of the labeled histidine groups of albumin and a spin labeled steroid. The distance was estimated as **r** > 1.8 nm. Changes of albumin molecule caused by binding steroids had allosteric character and corresponded to the trans-globular effects.

Study of the location of spin-labeled thiol groups relatively the active center of Ca-depending ATP-ase, in which diamagnetic Ca(II) ions were substituted with paramagnetic Mn(II) ions, allowed estimate the distance between the label and manganese ion as 1.1 nm (Maksina et al., 1979.

Later, at the end of 20th and beginning of 21st century, when new, informative, and modern quantitative methods based on double electron-electron resonance (ELDOR) and high frequency EPR spectroscopy were created as well as new methodologies. For example, measurement of the distance between two spin labels in proteins permits distinguish the spatial orientation of elements of defined secondary structure (Hustedt & Beth, 1999). By using site-directed spin labeling, it is possible to determine multiple distance values and thereby build tertiary and quaternary structural models as well as measure the dynamics of structural changes. New analytical methods for determining interspin distances and relative orientations for uniquely oriented spin labels have been developed using global analysis of multifrequency EPR data. New methods have also been developed for determining interprobe distances for randomly oriented spin labels. These methods are being applied to a wide range of structural problems, including peptides, soluble proteins, and membrane proteins, that are not readily characterized by other structural techniques (Hustedt & Beth, 1999). Nevertheless, a simple-measured d_1/d parameter was used rather often during these years.

By using a variety of biochemical and biophysical approaches, a helix packing model for the lactose permease of *Escherichia coli* has been proposed (He et al., 1997). The four residues that are irreplaceable with respect to coupling were paired: Glu269 (helix VIII) with His322 (helix X) and Arg302 (helix XI) with Glu325 (helix X). In addition, the substrate translocation pathway was located at the interface between helices V and VIII, which is in close vicinity to the four essential residues. Based on this structural information and functional studies of mutants in the four irreplaceable residues, a molecular mechanism for energy coupling in the permease has been proposed. It was shown by two methods that Arg302 is also close to Glu269. Glu269-His, Arg302-His, and His322-Phe binds Mn^{2+} with high affinity at pH 7.5, but not at pH 5.5. Site-directed spin-labeling of the double Cys mutant Glu269-Cys / Arg302-Cys exhibited spin-spin interaction with an interspin distance of about 1.4-1.6 nm. The spin-spin interaction was stronger and interspin distance shorter after the permease was reconstituted into proteoliposomes. Taken as a whole, the data were consistent with the idea that Arg302 may interact with either Glu325 or Glu269 during turnover (He et al., 1997).

Hess et al., 2002, have studied the secondary structure, subunit interaction, and molecular orientation of vimentin molecules within intact intermediate filaments and assembly intermediates. Spectroscopy data proved α-helical coiled-coil structures at individual amino acids 316–336 located in rod 2B. Analysis of positions 305, 309, and 312 identify this region as conforming to the helical pattern identified within 316–336 and thus demonstrated that this region is in an α-helical conformation. Varying the position of the spin label, authors could identify both intra- and inter-dimer interactions. With a label attached to the outside of the α-helix, it have been able to measure interactions between positions 348 of separate dimers as they align together in intact filaments, identifying the exact point of overlap. By mixing different spin-labeled proteins, Hess et al. demonstrated that the interaction at position 348 is the result of

an anti-parallel arrangement of dimers. This approach provided high resolution structural information (<2 nm resolution), can be used to identify molecular arrangements between subunits in an intact intermediate filament, and should be applicable to other noncrystallizable filamentous systems as well as to the study of protein fibrils (Hess et al., 2002).

Continuing the approach established the utility of site-directed spin labeling and EPR to determine structural relationships among proteins in intact intermediate filaments Hess et al., 2004, have introduced spin labels at 21 residues between amino acids 169 and 193 in rod domain 1 of human vimentin. The EPR spectra provided direct evidence for the coiled coil nature of the vimentin dimer in this region. This result was consistent with predictions but had never been experimentally demonstrated previously. Previously it was identified that residue 348 in the rod domain 2 acted as one point of overlap between adjacent dimers in intact filaments, and a new study was defined residue 191 in the rod domain 1 as a second point of overlap and established that the dimers are arranged in the anti-parallel and staggered orientation at this site. These results are shown in Table 7. By isolating spin-labeled

Position	184	189	190	191	192			
d_1/d [a]	0.33	0.47	0.42	0.45	0.49			
Δ	0.01	0.15	0.1	0.13	0.17			
<r>, Å	> 25	14.5	17.0	15.3	13.9			
Position	281	282	283	284	285	286	287	288
d_1/d [b]	0.43	0.38	0.63	0.44	0.43	0.40	0.45	0.46
Δ	0.11	0.06	0.31	0.12	0.11	0.08	0.13	0.14
<r>, Å	16.3	22.0	11.9	15.7	16.3	18.9	15.3	14.9
Position	289	290	291	292	293	294	295	296
d_1/d [b]	0.39	0.43	0.71	0.38	0.41	0.48	0.44	0.43
Δ	0.07	0.11	0.39	0.06	0.09	0.16	0.12	0.11
<r>, Å	20.2	16.3	11.4	22.0	17.8	14.2	15.7	16.3
Position	297	298	299	300	301	302	304	
d_1/d [b]	0.43	0.51	0.50	0.43	0.48	0.59	0.39	
Δ	0.11	0.19	0.18	0.11	0.16	0.27	0.07	
<r>, Å	16.3	13.4	13.7	16.3	14.2	12.3	20.2	
Position	323	324	325	326	327	328	329	330
d_1/d [c]	0.48	0.33	0.32	0.46	0.34	0.38	0.33	0.49
Δ	0.16	0.01	-	0.14	0.02	0.06	0.01	0.17
<r>, Å	14.2	> 25	-	14.9	> 25	22.0	> 25	13.9
Position	331	332	333	334	335	336		
d_1/d [c]	0.34	0.35	0.46	0.34	0.33	0.33		
Δ	0.02	0.03	0.14	0.02	0.01	0.01		
<r>, Å	> 25	> 25	14.9	> 25	> 25	> 25		

Table 7. Calculation of distances <**r**> between spin labels at different positions in Vimentin by d_1/d parameter measured from spectra recorded at –100°C in (Hess, [a] 2004, [b] 2006, [c] 2002)

samples at successive stages during the dialysis that lead to filament assembly *in vitro*, authors established a sequence of interactions that occurs during *in vitro* assembly, starting with the α-helix and loose coiled coil dimer formation. Then the formation of tetrameric species centered on residue 191, followed by interactions centered on residue 348 suggestive of octamer or higher order multimer formation. A continuation of this strategy by the authors revealed that both 191–191 and 348–348 interactions were present in low ionic strength Tris buffers when vimentin was maintained at the "protofilament" stage of assembly (Hess et al., 2004).

Mutations in intermediate filament protein genes were responsible for a number of inherited genetic diseases including skin blistering diseases, corneal opacities, and neurological degenerations. It was shown that mutation of the arginine (Arg) residue to be causative in inherited disorders in at least four different intermediate filament (IF) proteins found in skin, cornea, and the central nervous system. Thus this residue is very important to IF assembly and/or function. The impact of mutation at this site in IFs was investigated by spin labeling. Compared with wild type vimentin, the mutant showed normal formation of the coiled coil dimers, with a slight reduction in the stability of the dimer in rod domain 1. Probing the dimer-dimer interactions showed the formation of normal dimer centered on residue 191 but a failure of dimerization at residue 348 in rod domain 2. These data revealed a specific stage of assembly at which a common disease-causing mutation in IF proteins interrupts assembly (Hess et6 al., 2005).

Site-directed spin labeling, EPR and d_1/d parameter were logically used to probe residues 281-304 of human vimentin, a region that has been predicted to be a non-α-helical linker and the beginning of coiled-coil domain 2B (Hess et al., 2006). This region has been hypothesized to be flexible with the polypeptide chains looping away from one another. EPR analysis of spin-labeled mutants indicated that several residues reside in close proximity, suggesting that adjacent linker regions in a dimer run in parallel. Also, the polypeptide backbone was relatively rigid and inflexible in this region. This region did not show the characteristics of a coiled-coil as has been identified elsewhere in the molecule. Within this region, spectra from positions 283 and 291 were unique from all others of the examined. Structural parameters are given in Table 7. These positions displayed a significantly stronger interaction than the contact positions of coiled-coil regions. Analysis of the early stages of assembly by dialysis from 8 M urea and progressive thermal denaturation showed the close apposition and structural rigidity at residues 283 and 291 occurs very early in assembly, well before coiled-coil formation in other parts of the molecule. Spin labels placed further downstream demonstrated EPR spectra suggesting that the first regular heptad of rod domain 2 begins at position 302. In conjunction with previous characterization of region 305-336 by the same authors and the solved structure of rod 2B from 328-405, the full extent of coiled-coil domain in rod 2B became now known, spanning from vimentin positions 302-405 (Hess et al., 2006).

Phosphorylation processes drove the disassembly of the vimentin intermediate filament (IF) cytoskeleton at mitosis. Data of chromatographic analysis have suggested that phosphorylation produced a soluble vimentin tetramer, but little has been determined about

the structural changes that were caused by phosphorylation or the structure of the resulting tetramer. Pittenger et al., 2008, have studied site-directed spin labeling and EPR for examining the structural changes resulting from protein kinase A phosphorylation of vimentin IFs in vitro. EPR spectra suggested that the tetrameric species resulting from phosphorylation are the A11 configuration. It was also established that the greatest degree of structural change was connected with the linker 2 and the C-terminal half of the rod domain, despite the fact that most phosphorylation occurs in the N-terminal head domain. The phosphorylation-induced changes notably affected the proposed "trigger sequences" located in the linker 2 region. These data were the first to document specific changes in IF structure resulted from a physiologic regulatory mechanism and provided further evidence that the linker regions play a key role in IF structure and regulation of assembly-disassembly processes (Pittenger et al., 2008).

Four doubly spin-labeled variants of human carbonic anhydrase II and corresponding singly labeled variants were prepared by site-directed spin labeling (Persson et al., 2001). The distances between the spin labels were obtained from CW X-band EPR spectra by analysis of the relative intensity of the half-field transition, Fourier deconvolution of line-shape broadening, d_1/d parameter, and computer simulation of line-shape changes. Distances also were determined by four-pulse double electron-electron resonance. For each variant, at least two methods were applicable and reasonable agreement between methods was obtained. Distances ranged was from 7 to 24 Å. The doubly spin-labeled samples contained some singly labeled protein due to incomplete labeling. The sensitivity of each of the distance determination methods to the non-interacting component was compared (Persson et al., 2001).

The C-terminal end of ubiquitin (Ub) was covalently attached to the amino group of a lysine in a target protein (Steinhoff, 2002). Additional ubiquitin groups were added using Ub-Ub linkages to form a polyubiquitin chain. The accessibility and the molecular dynamics of the target domain for each protein substrate was expected to be distinctive and in this article the author investigated the ubiquitination mediated protein turnover by means of site-directed spin labeling. EPR data were obtained and interpreted in terms of secondary and tertiary structure resolution of proteins and protein complexes. Analysis of the spin labeled side chain mobility, its solvent accessibility, the polarity of the spin label micro-environment and distances between spin labels allowed to model protein domains or protein-protein interaction sites and their conformational changes with a spatial resolution at a reasonable level. The structural changes accompanying protein function or protein-protein interaction were monitored in the millisecond time range (Steinhoff, 2002).

Using modern pulse and multi-frequency techniques combined with site-directed spin labeling and EPR spectroscopy, the protein-protein and protein-oligonucleotide interaction was studied (Steinhoff, 2004). Analysis of the spin label spectra provided information about distances between spin labels and allowed the modeling of protein-protein interaction sites and their conformational changes. Structural changes were detected with millisecond time resolution. Inter- and intra-molecular distances were

determined in the range from approximately 0.5 to 8.0 nm by the combination of CW and pulse EPR methods (Steinhoff, 2004).

The elucidation of structure and function of proteins and membrane proteins by EPR spectroscopy has become increasingly important in recent years because of new approaches of spectroscopic methods and in the chemistry of nitroxide spin labels. These new developments have increased the demand for tailor-made amino acids carrying a spin label on the one hand and for reliable methods for their incorporation into proteins on the other. Becker et al., 2005, described methods for site-specific spin labeling of proteins and showed that a combination of recombinant synthesis of proteins with chemically produced peptides (expressed protein ligation) allowed the preparation of site-specifically spin-labeled proteins.

Apolipoprotein A-I (apoA-I) is the major protein constituent of high density lipoprotein (HDL) and plays a central role in phospholipid and cholesterol metabolism. This 243-residue long protein is remarkably flexible and assumes numerous lipiddependent conformations. Using EPR spectroscopy of site-directed spin labels in the N-terminal domain of apoA-I (residues 1–98), Lagerstedt et al., 2007, have mapped a mixture of secondary structural elements, the composition of which was consistent with findings from other methods. Based on side chain mobility, the precise location of secondary elements for amino acids 14–98 was determined for both lipid-free and lipid-bound apoA-I. Based on intermolecular dipolar coupling at positions 26, 44, and 64, and d_1/d measurements, these secondary structural elements were arranged into a tertiary fold to generate a structural model for lipid-free apoA-I in solutions (Lagerstedt et al., 2007).

Site-directed spin labeling and EPR spectroscopy were used for determining the structure of proteins and its conformational changes and dynamics of membrane proteins at physiological conditions. Analysis of these approaches is given in a review written by Czogalla et al., 2007.

β-spectrin is responsible for interactions with ankyrin. Structural studies indicated that this system exhibits a mixed 310/α-helical conformation and is highly amphipathic. The mechanism of its interactions with biological membranes was investigated with a series of singly and doubly spin-labeled erythroid β-spectrin-derived peptides (Czogalla et al., 2008). The spin-label mobility and spin–spin distances were analyzed via EPR spectroscopy, d_1/d parameter, and two different calculation methods. The results indicated that in β-spectrin, the lipid-binding domain, which is part of the 14th segment, has the topology of typical triple-helical spectrin repeat, and it undergoes significant changes when interacting with phospholipids or detergents. A mechanism for these interactions was proposed (Czogalla et al., 2008).

Halorhodopsin from *Natronomonas pharaonis* (pHR) is a light-driven chloride pump that transports a chloride anion across the plasma membrane following light absorption by a retinal chromophore which initiates a photocycle. Analysis of the amino acid sequence of pHR revealed three cysteine (Cys) residues in helices D and E. The Cys residues were

labeled with nitroxide radicals and studied using EPR spectroscopy. Labels mobility, accessibility to various reagents, and the distance between the labels have been studied (Mevorat-Kaplan et al., 2006). It was revealed by following the d_1/d parameter that the distance between the spin labels is ca. 13-15 Å. The EPR spectrum suggested that one label had a restricted mobility while the other two were more mobile. Only one label was accessible to hydrophilic paramagnetic broadening reagents leading to the conclusion that this label was exposed to the water phase. All three labels were reduced by ascorbic acid and reoxidized by molecular oxygen. It was found that the protein experiences conformation alterations in the vicinity of the labels during the pigment photocycle. It was suggested that Cys186 is exposed to the bulk medium while Cys184, located close to the retinal ionone ring, exhibits an immobilized EPR signal and is characterized by a hydrophobic environment (Mevorat-Kaplan et al., 2006).

Alliinase, an enzyme found in garlic, catalyzes the synthesis of the well-known chemically and therapeutically active compound allicin (diallyl thiosulfinate). The enzyme is a homodimeric glycoprotein that belongs to the fold-type I family of pyridoxal-50-phosphate-dependent enzymes. There are 10 cysteine residues per alliinase monomer, eight of which form four disulfide bridges and two are free thiols. Cys368 and Cys376 form a SAS-bridge located near the C-terminal and plays an important role in maintaining both the rigidity of the catalytic domain and the substrate-cofactor relative orientation. Weiner et al., 2009, demonstrated that the chemical modification of allinase with the colored ASH reagent yielded chromophore-bearing peptides and showed that the Cys220 and Cys350 thiol groups are accessible in solution. EPR kinetic measurements using disulfide containing a stable nitroxyl biradical showed that the accessibilities of the two ASH groups in Cys220 and Cys350 differ. The enzyme activity and protein structure (measured by circular dichroism) were not affected by the chemical modification of the free thiols. The d_1/d measurements and its calibration curve on distances obtained by authors gave a distance value between Cys220 and Cys350 >2.2 nm; this is in good agreement with known structural data. Modification of the alliinase thiols with biotin and their subsequent binding to immobilized streptavidin enabled the efficient enzymatic production of allicin (Weiner et al., 2009).

New EPR spectroscopy methods allows now measuring distances reasonably larger 3.0 nm which are nor available for d_1/d method. Long-range structural information derived from paramagnetic relaxation enhancement observed in the presence of a paramagnetic nitroxide radical was used for structural characterization of globular, modular and intrinsically disordered proteins, as well as protein–protein and protein-DNA complexes (Gruene et. al., 2011). The authors characterized the conformation of a spin-label attached to the homodimeric protein CylR2 using a combination of X-ray crystallography, EPR and NMR spectroscopy. Close agreement was found between the conformation of the spin label observed in the crystal structure with interspin distances measured by EPR and signal broadening in NMR spectra. It was suggested that the conformation seen in the crystal structure was also preferred in solution. In contrast, conformations of the spin label observed in crystal structures of T4 lysozyme was not in agreement with the paramagnetic relaxation enhancement observed for spin-labeled CylR2 in solution. These data

demonstrated that accurate positioning of the paramagnetic center is essential for high-resolution structure determination (Gruene et. al., 2011).

Rabenstein & Shin, 1995, suggested a new elegant, rather precise but a little bit sophisticated EPR "spectroscopic ruler" which was developed using a series of α-helical polypeptides, each modified with two nitroxide spin labels. A synthesized oligopeptide consisted of 21 amino acids with the following a chain: Ac-AAAALAAAALAAAALAAAALA-NH_2, where Ac is acetyl, A is alanine, L - is lysine residue. A series of variants of these peptides in which two alanines were substituted to cysteines with various positions in the chain. In all examples below these numbers are started from the Ac-alanine terminal. The EPR line broadening due to electron-electron dipolar interactions in the frozen state was determined using the Fourier deconvolution method. The dipolar spectra were then used to estimate the distances between the two nitroxides separated by non-labeled amino acids. Results agreed well with a simple α-helical model. The standard deviation from the model system was 0.09 nm in the range of 0.8-2.5 nm. The authors concluded that this technique can be applied to complex systems such as membrane receptors and channels, which are difficult to access with high-resolution NMR or X-ray crystallography, and will be particularly useful for systems for which optical methods are hampered by the presence of light-interfering membranes or chromophores (Rabenstein & Shin, 1995). Indeed, this method was used in several works during last ten years. We have carefully analyzed the data obtained by Rabenstein & Shin, 1995, and compared them with those determined with d_1/d method. Results are shown in Table 8.

Label positions	(6, 12)	(4, 8)	(4, 9)	(4, 11)	(4, 13)	(4, 17)
R, nm	1.46	0.91	1.46	1.00	1.79	2.35
d_1/d	0.49	1.17	0.48	0.69	0.45	0.41
r, nm	1.57	0.99	1.63	1.17	1.89	2.85

Table 8. The interspin distances measured by Rabenstein & Shin, 1995 (R), and from d_1/d parameter (**r**) for different double spin-labeled oligopeptides

The experimental interspin distances R measured by Rabenstein & Shin, 1995, were taken from their Fig. 5 of the article. d_1/d values for all biradicals as well as for a polypeptide with only one spin-labeled cysteine in the 6-th position, $(d_1/d)_0$ value equal to 0.37, we measured from the original EPR spectra shown in Fig. 2 of the article. Interspin distances **r** calculated by Eq. (26) using a parameter Δ, are given in Table 8. We could not use d_1/d parameter for polypeptides (6, 7) and (6, 8) because in their spectra the dipolar splitting of EPR lines are well-defined, and for the (6, 9) system the distance R is too short and a d_1/d value can not be measured. For other six biradical polypeptides (Table 8), one can conclude that R and **r** values are in reasonably good agreement (not worse than ± 0.1 nm) with systematically larger (~0.1 nm) values of **r**, probably because we used EPR spectra printed in the article, and not the original ones. All procedure of estimation **r** values took about one hour, while more precise but more complicated calculations by Rabenstein and Shin method take usually much longer time.

The interspin distances of two or more nitroxide spin labels attached to specific sites in insulins were determined for different conformations with application of EPR by the line broadening due to dipolar interaction (Steinhoff et al., 1997). The procedure was carried out by fitting simulated EPR powder spectra to experimental data, measured at temperatures below 200 K to freeze the protein motion. The experimental spectra were composed of species with different relative nitroxide orientations and interspin distances because of the flexibility of the spin label side chain and the variety of conformational substates of spin labeled insulins in frozen solution. Values for the average distance <r> and for the distance distribution width were determined from the characteristics of the dipolar broadened line shapes and d_1/d parameter. The resulting interspin distances determined for crystallized insulins in the R6 and T6 structure agreed well with structural data obtained by X-ray crystallography and by modeling of the spin-labeled samples. The EPR experiments revealed differences between crystal and frozen solution structures of the B-chain amino termini in the R6 and T6 states of hexameric insulins (Steinhoff et al., 1997). This study of interspin distances between attached spin labels applied to proteins is a nice example how to obtain structural information on proteins under conditions when other methods like two-dimensional NMR spectroscopy or X-ray crystallography are not applicable.

Gramicidin A was studied by CW-EPR and by double-quantum coherence electron paramagnetic resonance (DQC-EPR) in several lipid membranes (Dzikovski et al., 2004). Samples used were macroscopically aligned by isopotential spin-dry ultracentrifugation and vesicles. The nitroxide spin label was attached at the C-terminus yielding the spin-labeled product (GAsl). EPR spectra of aligned membranes containing GAsl showed strong orientation dependence. In DPPC and DSPC membranes at room temperature had the spectral shape consistent with high ordering, which, in conjunction with the observed high polarity of the environment of the nitroxide label, was interpreted in terms of the nitroxide moiety being close to the membrane surface. In contrast, EPR spectra of GAsl in DMPC membranes indicated deeper embedding and tilt of the NO group. The GAsl spectrum in the DPPC membrane at 35°C (the gel to P_β phase transition) exhibited sharp changes, and above this temperature became similar to that of DMPC. The dipolar spectrum from DQC-EPR clearly indicated the presence of pairs in DMPC membranes. This was not the case for DPPC, rapidly frozen from the gel phase but could be a hint of aggregation. The interspin distance in the pairs was determined as 3.09 nm, in good agreement with estimated for the head-to-head GAsl dimer (the channel-forming conformation), which matched the hydrophobic thickness of the DMPC bilayer (Dzikovski et al., 2004). Both DPPC and DSPC, apparently as a result of hydrophobic mismatch between the dimer length and bilayer thickness, did not favor the channel formation in the gel phase. In the P_β and L_α phases of DPPC (above 35°C) the channel dimmer was formed, as evidenced by the DQC-EPR dipolar spectrum after rapid freezing. A comparison with studies of dimer formation by other physical techniques indicated the desirability of using low concentrations of Gramicidin A accessible to the EPR methods for the study (Dzikovski et al., 2004).

Recently, Dzikovski et al., 2011, published experimental results on channel and nonchannel forms of Gramicidin A (GA) studied by EPR in various lipid environments using new mono- and double-spin-labeled compounds. For GA channels, it was demonstrated that pulse dipolar EPR allowed to determine the orientation of the membrane-traversing molecules relative to the membrane normal and to study small effects of lipid environment on the interspin distances in the spin-labeled GA channel. The nonchannel forms of GA were also studied by pulse dipolar EPR for determination of interspin distances corresponding to monomers and double-helical dimers of spin-labeled GA molecules in the organic solvents trifluoroethanol and octanol. The same distances were observed in membranes. Since detection of nonchannel forms in the membrane is complicated by aggregation, the authors suppressed any dipolar spectra from intermolecular interspin distances arising from the aggregates by using double-labeled GA in a mixture with excess unlabeled GA molecules. In hydrophobic mismatching lipids (L-phase of DPPC), GA channels have dissociated into free monomers. The structure of the monomeric form was found similar to a monomeric unit of the channel dimer. The double-helical conformation of gramicidin was also found in some membrane environments. It was revealed that in the gel phase of saturated phosphatidylcholines, the fraction of double-helices increased in the following order: DLPC < DMPC < DSPC < DPPC, and the equilibrium DHD/monomer ratio in DPPC was determined. In membranes, the double-helical form was presented only in aggregates. The effect of N-terminal substitution in the GA molecule upon channel formation was also studied (Dzikovski et al., 2011). This work has demonstrated how pulsed dipolar EPR can be used to study complex equilibria of peptides in membranes.

We would like to attract attention to a recent work by Gordon-Grossman et al., 2009, in which a combined pulse EPR and Monte Carlo simulation study provided the insight on peptide-membrane interactions and the molecular structure of the system. This new approach to obtain details on the distribution and average structure and locations of membrane-associated peptides successfully combined: a) PELDOR to determine intramolecular distances between spin labeled residues in peptides; b) electron spin echo envelope modulation (ESEEM) experiments for measuring water exposure and the direct interaction of spin labeled peptides with deuterium nuclei in the phospholipid molecules, and c) Monte Carlo simulations (MCS) to derive the peptide-membrane populations, energetics, and average conformation of the native peptide and mutants mimicking the spin labeling. The membrane-bound and solution state of the well-known antimicrobial peptide melittin, used as a model system was investigated, and a good agreement between the experimental results and the MCS simulations regarding the distribution of distances between the labeled amino acids, the side chain mobility, and the peptide's orientation was obtained, as well as for the extent of membrane penetration of amino acids in the peptide core. It was shown that the EPR data reported a deeper membrane penetration of the termini compared to the MCS simulations. In case of melittin adsorption on the membrane surface in a monomeric state, it was observed as an amphipatic helix with its hydrophobic residues in the hydrocarbon region of the membrane and its charged and polar residues in the lipid headgroup region (Gordon-Grossman et al., 2009).

8.2. Nucleic acids

EPR spectroscopy has been used broadly for investigating peculiarities of the structural organization and its transformation for DNA, RNA molecules, their models and different protein-nucleic acid complexes. A lot of works were published during last 45 years. Below, we will discuss only several of them relating to the topic of the chapter.

The study of DNA-dye interaction by the spin label method was carried out by Zavriev, et al., 1976. The binding of ethidium bromide and acriflavin dyes with DNA macromolecule modified with spin-labeled analogue of ethylene imine has been studied. These spin labels were shown to bind covalently to DNA, at the same time the number of the dye molecules bound to DNA was decreased without any changes of the binding constant. Analysis of EPR spectra of the samples in the frozen 50% water-glycerol mixture at 77 K for spin-labeled DNA has shown that addition of the dyes increased distances <r> between the labels, that was explained by the increase in DNA length upon formation of the complex with dye molecules. Structural data in the work were obtained from measuring d_1/d values (Zavriev, et al., 1976).

The use of d_1/d measurements for structural characterization of spin labeled DNA and RNA was also described in a review of EPR studies of the structure and dynamic properties of nucleic acids and other biological systems written by Kamzolova & Postnikova, 1981. When spin labels were attached to different sites of a macromolecule, the quantitative information could be obtained about conformational properties of these local regions and, as a result, about the functional behaviour of the systems.

A distance ruler for RNA using EPR and site-directed spin labeling (SDSL) has been suggested by Kim et al., 2004. The site-directed spin-labeled 10-mer RNA duplexes and HIV-1 TAR RNA motifs with various interspin distances were examined. HIV-1 TAR RNA is the binding site of the viral protein Tat, the trans-activator of the HIV-1 LTR. The long terminal repeat, LTR, regulates HIV-1 viral gene expression via its interaction with multiple viral and host factors. It is present at the 5'- end of all HIV-1 spliced and unspliced mRNAs in the nucleus as well as in the cytoplasm. SDSL was applied to RNA structural biology rather rare, despite an importance of knowledge of RNA structure and RNA-protein complex formation. As a model study for measuring distances in RNA molecules using continuous wave (CW) EPR spectroscopy, the spin labels were attached to the 2′-NH_2 positions of appropriately placed uridines in the duplexes, and interspin distances were measured from both molecular dynamics simulations (MDS) and Fourier deconvolution method (FDM) developed by Rabenstein & Shin, 1995. The 10-mer duplexes had interspin distances in the range from 1.0 to 3.0 nm by MDS estimations; however, dipolar line broadening of the CW EPR spectra was observed for the RNAs with interspin distances of 1.0 to 2.1 nm and not for distances over 2.5 nm. Unfortunately, the authors did not use the d_1/d method for the distance measurement, probably because this approach was described only in Russian language literature. Its application could add the necessary information to the subject, the more so the appropriate EPR spectra at low temperature were recorded. The conformational

changes in TAR (transactivating responsive region) RNA in the presence and in the absence of different divalent metal ions were monitored by measuring distances between two nucleotides in the bulge region. The predicted interspin distances obtained from the FDM method and those from MDS calculations match well for both the model RNA duplexes and the structural changes predicted for TAR RNA. These results demonstrate that distance measurement using EPR spectroscopy is a potentially powerful method to help predict the structures of RNA molecules (Kim et al., 2004).

Site-directed spin labeling measurements of nanometer distances in nucleic acids using a sequence-independent nitroxide probe has been carried out also in (Cai et al., 2006). Analysis of electron spin dipolar interactions between pairs of nitroxides yields the inter-nitroxide distance, which provides quantitative structural information. The PELDOR and NMR methods had enabled such distance measurements up to 7.0 nm in bio-molecules, thus opening up the possibility of SDSL global structural mapping. The study evaluated SDSL distance measurement using a nitroxide spin label that was attached, in an efficient manner, to a phosphorothioate backbone position at arbitrary DNA or RNA sequences. Radical pairs were attached to selected positions of a dodecamer DNA duplex with a known NMR structure, and eight distances, ranging from 2.0 to 4.0 nm, were measured using PELDOR technique. The measured distances correlated strongly ($R^2 = 0.98$) with the predicted values calculated based on a search of sterically allowable radical conformations in the NMR structure, and the accurate distance measurements was demonstrated. The method was proposed for global structural mapping of DNA and DNA–protein complexes (Cai et al., 2006).

The molecular chaperone DnaK recognizes and binds substrate proteins via a stretch of seven amino acid residues that is usually only exposed in unfolded proteins. The binding kinetics is regulated by the nucleotide state of DnaK, which alternates between DnaK and ATP (fast exchange) and DnaK and ADP (slow exchange). These two forms cycle with a rate mainly determined by the ATPase activity of DnaK and nucleotide exchange. The different substrate binding properties of DnaK were mainly attributed to changes of the position and mobility of a helical region in the C-terminal peptide-binding domain, the so-called LID (Popp et al., 2005). Authors investigated the nucleotide-dependent structural changes in the peptide-binding region and the question: could they induce structural changes in peptide stretches using the energy available from ATP hydrolysis. Model peptides contained two cysteine residues at varying positions and were derived from the structurally well-studied peptide NRLLLTG and labelled with spin probes. Measurements of distances between spin labels were carried out by EPR for free peptides or peptides bound to the ATP and ADP-state of DnaK, respectively. No significant change of distances between labels was observed, hence, no structural changes that could be sensed by the probes at the position of central leucine residues located in the center of the binding region occur due to different nucleotide states. It was concluded that the ATPase activity of DnaK is not connected to structural changes of the peptide-binding pocket but has an effect on the LID domain or other further remote residues (Popp et al., 2005).

A rigid, spin-labeled nucleoside was prepared using a convergent synthetic strategy that could also be applied for the synthesis of the corresponding ribonucleoside (Barhate et al., 2007). EPR spectroscopic analysis of a DNA that contained the rigid spin label verified its limited mobility within a DNA duplex. The rigid spin label had several advantages over previously reported spin labels for nucleic acids: a) distance measurements between two rigid spin labels can be done more accurate than between flexible nitroxides; b) possibility of determination of relative orientations of the two rigid labels, that thereby provided more detailed structural information; c) the nucleoside became fluorescent upon reduction of the nitroxide with a mild reducing agent, that was the first example of a spectroscopic probe that could be used for structural studies by both EPR and fluorescence spectroscopy. The dual spectroscopic activity of the spin label enabled the preparation of nucleic acids that contain a redox-active sensor in their structure. More detailed characterization of the new bifunctional spectroscopic probe and its application for the studies of the structure and dynamics of nucleic acids will be reported in due course (Barhate et al., 2007).

Schiemann et al., 2007, described the facile synthesis of the nitroxide spin-label 2,2,5,5-tetramethyl-pyrrolin-1-oxyl-3-acetylene, TPA, and its binding to DNA/RNA through Sonogashira cross-coupling during automated solid-phase synthesis. They also have measured distance between two such spin-labels on RNA/DNA using PELDOR, and suggested to use this approach for studying global structure elements of oligonucleotides in frozen solutions at RNA/DNA amounts of ~10 nmol. The procedure suggested by authors should be applicable to RNA/DNA strands of up to ~80 bases in length and PELDOR yields reliably spin–spin distances up to ~6.5 nm (Schiemann et al., 2007).

Indeed, over the last 10 years PELDOR has emerged as a powerful new biophysical method without size restriction to the biomolecule under studying, and has been applied to a large variety of nucleic acids as well as proteins and protein complexes in solution or within membranes. Small nitroxide spin labels, paramagnetic metal ions, amino acid radicals or intrinsic clusters and cofactor radicals have been already used as spin centres (Reginsson & Schiemann, 2011).

8.3. Biomembranes and lipid-protein complexes

Native biological membranes and their chemical models such as vesicles and lipid double-layered membranes (emulsions) as well as various lipid-protein complexes are a huge class of objects suitable for investigation by spin probe/label technique. Structural results obtained by EPR for the third group (lipid-protein complexes) were discussed in Section 8.1 of this review. Numerous articles were published during last 50 years concerning biomembranes but only very few were related to quantitative measurements of the local concentration of spin probes and interspin distances. The main problem in such studies of the structural organization of biological membranes is that when spin probes (nitroxide radicals) are penetrated into outer or inner layer of the double-layered membrane, they promptly become distributed in both layers of the membrane because of flip-flop transitions

(Berliner, 1976, Kuznetsov, 1976, Likhtenshtein et al., 2008, Hemminga & Berliner, 2007, Webb, 2006). Therefore, it is usually quite difficult to distinguish between dipolar coupling of spins inside one lipid layer or between spins localized in two lipid monolayers.

9. Conclusion

Measurement of distances or local concentrations in physical and macromolecular chemistry, solid state chemistry, molecular biology and biophysics is an important quantitative tool for investigating structure, spatial organization and conformational transitions in solids, solid solutions, polymers, biological macromolecules, and complex supramolecular systems using site-directed spin labeling and various techniques of EPR spectroscopy. Modern approaches of EPR such as high frequency/high field EPR, pulce technique and double resonances, dipolar EPR spectroscopy allow researchers determine not only interspin distances but also their relative 3-D orientation and the behaviour of these complex systems under their functioning using stable nitroxide radicals. Analysis of the results obtained shows that became a method making possible controlling quantitatively spatial structure and properties of chemical and biological systems in conditions the most close to natural. And this is very important for correct understanding of the mechanisms of these processes.

Scientific progress is irreversible. During the last forty years three generations of researchers were changed, and naturally the development of new modern methods of quantitative investigation is continuously in progress. These methods are usually correct, informative but very technically complex and need a lot of theoretical and computer calculations, i.e. take a lot of time. Therefore, such simple method as d_1/d parameter for estimation distances **r** in the case of pairwise distribution of nitroxide radicals and local concentrations C_{loc} or mean local distances <r> at their random (chaotic) distribution of paramagnetic centres can provide valuable structural information at the beginning serious complex and long-time investigation. Measurements of d_1/d values are simple and do not need much time especially considering important information provided by it. Evidently, d_1/d parameter should be used in the distance or concentration intervals and experimental conditions in which it determination is correct.

Author details

Alexander I. Kokorin
N.Semenov Institute of Chemical Physics RAS, Moscow, Russian Federation

Acknowledgement

The author thanks the Russian Foundation for Basic Research (grant 12-03-00623_a) for financial support of the work. I thank also Mrs. A. A. Goncharova, Mr. O. I. Gromov and Dr. I. A. Kokorin for their technical assistance in Chapter preparation.

10. References

Abragam, A. (1961). *The principles of nuclear magnetism*, Clarendon Press, Oxford

Aleksandrova, T. A.; Wasserman, A. M.; Medvedeva, T. V.; Shapiro, A. M. & Korshak, Yu. V. (1986). The intramolecular mobility and local density of links in nitroxide polyradicals based on styrene co-polymers with maleic anhydride. *Vysokomolec. Soed. B*, Vol. 28, No. 11, 832-835, ISSN: 0507-5475

Altshuler, S. A. & Kozirev, B. M. (1964). *Electron Paramagnetic Resonance*, Academic Press, New York

Barhate, N.; Cekan, P.; Massey, A. P. & Sigurdsson, S. Th. (2007). A nucleoside that contains a rigid nitroxide spin label: A fluorophore in disguise, *Angew. Chem. Int. Ed.*, Vol. 46, No. 15, 2655 –2658, ISSN 1433-7851

Bender, C. J. & Berliner, L. J., Eds. (2006). *Computational and Instrumental Methods in EPR*, in *Biological Magnetic Resonance*, Vol.25, Springer Verlag, ISBN: 0-387-33145-X

Becker, C. F. W.; Lausecker, K.; Balog, M.; Kalai, T.; Hideg, K.; Steinhoff, H.-J. & Engelhard, M. (2005). Incorporation of spin-labelled amino acids into proteins. *Magn. Reson. Chem.*, Vol. 43, S34–S39, ISSN 0749-1581

Berliner, L. J. (1976). *Spin Labeling: Theory and Applications*. Academic Press, ISBN 0-120-92350-5, New York

Berliner, L. J. (1979). *Spin Labeling II: Theory and Applications*. Academic Press, ISBN 0120923505, New York

Berliner, L. J.; Eaton, S. S. & Eaton, G. R., Eds (2001). *Distance Measurements in Biological Systems by EPR*. In *Biological Magnetic Resonance*, Vol. 19. Springer Verlag, ISBN: 0-306-46533-7, New York, London

Bird, G. H.; Pornsuwan, S.; Saxena, S. & Schafmeister, C. E. (2008). Distance distributions of end-labeled curved bispeptide oligomers by E. S. R. *ACS Nano*, Vol. 2, No. 9, 1857–1864, ISSN 1936-0851

Blumenfeld, L. A.; Voevodskii, V. V. & Semenov, A. G. (1962). *Application of Electron Paramagnetic Resonance in Chemistry*, Nauka, Novosibirsk

Bravaya, N. M. & Pomogailo, A. D. (2000). Spin labels as the instrument for analysis of topochemistry of polymer-immobilized Ziegler catalytic systems. *J. Inorg. Organomet. Polymers*, Vol. 10, No. 1, 1-22, ISSN 1053-0495

Brustolon, M. R. & Giamello E., Eds. (2009). *Electron Paramagnetic Resonance Spectroscopy: A Practitioner's Toolkit*, Wiley, ISBN-10: 0-4702-5882-9

Buchachenko, A. L. & Wasserman, A. M. (1973). *Stable Radicals*, Khimiya, Moscow. *(*1976). *Stable Radicals*. Wiley, ISBN 9067642592, *London*

Cai, Q.; Kusnetzow, A. K.; Hubbell, W. L.; Haworth, I. S.; Gacho, G. P. C.; Van Eps, N.; Hideg, K.; Chambers, E. J. & Qin, P. Z. (2006). Site-directed spin labeling measurements of nanometer distances in nucleic acids using a sequence-independent nitroxide probe. *Nucleic Acids Research*, Vol. 34, No. 17, 4722-4730, ISSN 0305-1048

Capiomont, A. (1972). Structure cristalline du radical nitroxyde: subérate de di(tétraméthyl-2,2,6,6 pipéridinyl-4 oxyle-1). *Acta Cryst. B*, Vol. B28, No. 7, 2298-2301, ISSN 0567-7408

Czogalla1, A.; Pieciul, A.; Jezierski, A. & Sikorski, A. F. (2007a). Attaching a spin to a protein — site-directed spin labeling in structural biology, *Acta Bioch. Polonica*, Vol. 54, No. 2, 235–244, ISSN 0001-527X

Czogalla a, A.; Grzymajło a, K.; Jezierski, A. & Sikorski, A. F. (2008). Phospholipid-induced structural changes to an erythroid β spectrin ankyrin-dependent lipid-binding site Biochimica et Biophysica Acta, Vol. 1778, No. 11, 2612–2620, ISSN 0005-2736

Dubinskii, A. A.; Grinberg, O. Ya.; Tabachnik, A. A.; Shapiro, A. B.; Ivanov, V. P.; Rozantsev, E. G. & Lebedev, Ya. S. (1974). The measurement of distances between paramagnetic fragments in biradicals by the forbidden transition $\Delta M_S=2$. *Biofizika*, Vol. 19., No. 5, 840-842, ISSN 0006-3029

Dzikovski, B. G.; Borbat, P. P. & Freed, J. H. (2004). Spin-labeled Gramicidin A: Channel formation and dissociation. *Biophys. J.*, Vol. 87, No. 5, 3504-3517, ISSN 0006-3495

Dzikovski, B. G.; Borbat, P. P. & Freed, J. H. (2011). Channel and Nonchannel Forms of Spin-Labeled Gramicidin in Membranes and Their Equilibria. *J. Phys. Chem. B*, Vol. 115, No. 1, 176-185, ISSN 1520-6106

Eaton, S. S. & Eaton, G. R. (2001a). Relaxation times of organic radicals and transition metal ions. In: *Distance Measurements in Biological Systems by EPR*. In *Biological Magnetic Resonance*, (2001), Berliner, L. J.; Eaton, S. S. & Eaton, G. R., Eds. Vol. 19, 29-154, Springer Verlag, ISBN: 0-306-46533-7, New York, London

Eaton, S. S. & Eaton, G. R. (2001b). Determination of distances based on T_1 and T_m effects. In: *Distance Measurements in Biological Systems by EPR*. In *Biological Magnetic Resonance*, (2001), Berliner, L. J.; Eaton, S. S. & Eaton, G. R., Eds. Vol. 19, 348-382, Springer Verlag, ISBN: 0-306-46533-7, New York, London

Eaton, S. S. & Eaton, G. R. (2004). *Measurements of Interspin Distances by EPR*. In: *Electron Paramagnetic Resonance*, Vol. 19, 318-337, ISBN: 0-306-46533-7

Eaton, G. R.; Eaton, S. S.; Barr, D. P. & Weber, R. T. (2010). *Quantitative EPR*. Springer, ISBN 978-3211929476,

Elek, G.; Sajgo, M.; Grigorian, G. L.; Chibrikin, V. M. &Keleti, T. (1972). Spin labelling of D-glyceraldehyde-3-phosphate Dehydrogenase with specific reagents. *Acta Biochim. et Biophys. Acad. Sci. Hung.*, Vol. 7, No. 2, 119-131, ISSN 0237-6261

Fielding, L.; More, K. M.; Eaton, G. R. & Eaton, S. S. (1986). Metal-nitroxyl interactions. 46. Spectra of low-spin Iron(III) complexes of spin-labeled tetraphenylporphyrines and their implications for the interpretation of EPR spectra of spin-labeled Cytochrome P450. *J. Am. Chem. Soc.*, Vol. 108, No. 3, 618-625, *ISSN* 0002-7863

Filatova, M. P.; Reissmann, Z.; Reutova, T. O.; Ivanov, V. T.; Grigoryan, G. L.; Shapiro, A. M. & Rozantsev, E. G. (1977). Conformational states of bradykinin and its analogs in solution. III. ESR spectra of spin-labeled analogs. *Bioorg. Khimiya*, Vol. 3, No. 9, 1181-1189, ISSN 0132-3423

Flory, P. J. (1969). *Statistical Mechanics of Chain Molecules*. Wiley, ISBN 0-470-26495-0; reissued 1989, ISBN 1-56990-019-1, New York

Gordon-Grossman, M.; Gofman, Y.; Zimmermann, H.; Frydman, V.; Shai, Y.; Ben-Tal, N. & Goldfarb, D. (2009). A combined pulse EPR and Monte Carlo simulation study provides

molecular insight on peptide-membrane interactions. *J. Phys. Chem. B*, Vol. 113, No. 38, 12687–12695, ISSN 1089-5647

Grinberg, O. & Berliner, L. J., Eds. (2011). *Very High Frequency (VHF) ESR/EPR*, Springer, ISBN 978-1441934420,

Grinberg, O. Ya.; Nikitaev, A. T.; Zamaraev, K. I. & Lebedev, Ya. S. (1969). Influence of the concentration on the EPR line width in solid solutions of VO^{2+} and MoO^{3+}. *Zh. Strukt. Khimii,* Vol. 10, No. 2, 230-233, ISSN 0136-7463

Gruene, T.; Cho, M.-K.; Karyagina, I.; Kim, H.-Y.; Grosse, C.; Giller, K.; Zweckstetter, M. & Becker, S. (2011). Integrated analysis of the conformation of a protein-linked spin label by crystallography, EPR and NMR spectroscopy. *Biomol. NMR*, Vol. 49, No. 1, 111–119, ISSN 0925-2738

Hanson, G. & Berliner, L. J., Eds., (2010). *Metals in Biology: Applications of High-Resolution EPR to Metalloenzymes*, in: *Biological Magnetic Resonance*, Vol. 29, Springer, ISBN 978-1441911384,

He, M. M.; Voss, J.; Hubbell, W. L. & Kaback, H. R. (1997). Arginine 302 (Helix IX) in the lactose permease of *Escherichia coli* is in close proximity to Glutamate 269 (Helix VIII) as well as Glutamate 325 (Helix X). *Biochemistry*, Vol. 36, No. 44, 13682-13687, ISSN 0001527X

Hemminga, M. A. & Berliner, L. J., Eds. (2007). *ESR Spectroscopy in Membrane Biophysics*, in *Biological Magnetic Resonance*. Vol. 27, Springer Verlag 2007. ISBN: 0-387-25066-2.

Hess, J. F.; Voss, J. C. & FitzGerald, P. G. (2002). Real-time observation of coiled-coil domains and subunit assembly in intermediate filaments. *J. Biol. CChem.*, Vol. 277, No. 38, 35516–35522, ISSN 0021-. 9258

Hess, J. F.; Budamagunta, M. S.; Voss, J. C. & FitzGerald, P. G. (2004). Structural characterization of Human Vimentin Rod 1 and the sequencing of assembly steps in intermediate filament formation *in vitro* using site-directed spin labeling and EPR. *J. Biol. CChem.*, Vol. 279, No. 43, 44841–44846, ISSN 0021-. 9258

Hess, J., Budamagunta, M., FitzGerald, P., Voss, J. (2005). Characterization of structural changes in vimentin bearing an EBS-like mutation using site directed spin labeling and electron paramagnetic resonance, *J. Biol. Chem.*, Vol. 280, No. 3, 2141-2146, ISSN 0021-. 9258

Hess, J. F.; Budamagunta, M. S.; Shipman, R. L.; FitzGerald, P. G. & Voss, J. C. (2006). Characterization of the linker 2 region in human Vimentin using site-directed spin labeling and EPR. *Biochemistry*, Vol. 45, No. 39, 11737-11743, ISSN 0001527X

Hustedt, E. J. & Beth, A. H. (1999). Nitroxide spin-spin interactions: Applications to protein structure and dynamics. *Ann. Rev. Biophys. Biomol. Struct.*, Vol. 28, No. 1, 129-153, ISSN 1056-8700

Ionita, P.; Caragheorgheopol, A.; Gilbert, B. C. & Chechik, V. (2004). Mechanistic study of a place-exchange reaction of Au nanoparticles with spin-labeled disulfides. *Langmuir*, Vol. 20, 11536-11544. *ISSN* 0743-7463

Ionita, P.; Caragheorgheopol, A.; Gilbert, B. C. & Chechik, V. (2005). Dipole-dipole interactions in spin-labeled Au nanoparticles as a measure of interspin distances. *J. Phys. Chem. B*, Vol. 109, 3734-3742 *ISSN* 1089-5647

Ionita, P.; Volkov, A.; Jeschke, G. & Chechik, V. (2008). Lateral diffusion of thiol ligands on the surface of Au nanoparticles: An EPR study. *Anal. Chem.*, Vol. 80, No. 1, 95-106, *ISSN* 0003-2700

Ivanov, V. T.; Filatova, M. P.; Reissmann, Z.; Reutova, T. O.; Kogan, U. A.; Efremov, E. S.; Ivanov, V. S.; Galaktionov, S. G.; Grigoryan, G. L. & Bystrov, V. F. (1975a). The conformational states of bradykinin in solutions. *Bioorg. Khimiya*, Vol. 1, No. 8, 1241-1244, ISSN 0132-3423

Ivanov, V. T.; Filatova, M. P.; Reissmann, S.; Reutova, T. O.; Efremov, E. S.; Pashkov, V. S.; Galaktionov, S. G.; Grigoryan, G. L. & Ovchinnikov, Yu. A. (1975b). In: *Peptides: chemistry, structure and biology*, Walter, R. & Meienhofer, J., Eds. Ann Arbor Science, New York, 151-157.

Ivanov, V. T.; Miroshnikov, A. I.; Snezhkova, L. G.; Ovchinnikov, Yu. A.; Kulikov, A. V. & Likhtenstein, G. I. (1973). The application of EPR spectroscopy for studying conformational states of peptides. Gramicidine S. *Khimiya Prirod. Soed.* (Chemistry of Natural Compounds), Vol. 9, No. 1, 91-98, ISSN 0023-1150

Jeschke, G. (2002). Determination of the nanostructure of polymer materials by EPR spectroscopy. *Macromol Rapid Commun.*, Vol. 23, No. 2, 227-246, ISSN: 1521-3927

Kamzolova, S. G. & Postnikova, G. B. (1981). Spin-labelled nucleic acids. *Quart. Rev. Bioph.*, Vol. 14, No. 2, 223-288, ISSN 0033-5835

Khairutdinov, R. F. & Zamaraev, K. I. (1970). Study of the structure of frozen solutions with paramagnetic probes. Bull. Acad. Sci. USSR, Div. chemistry, No. 7, 1524-1528, ISSN 0002 3353

Khazanovich, T. N.; Kolbanovsky, A. D.; Kokorin, A. I.; Medvedeva, T. V. & Wasserman, A. M. (1992). EPR spectroscopy of spin-labeled macromolecules as a tool for determining chain conformations in amorphous solid polymers. *Polymer*, Vol. 33, No. 24, 5208-5214, ISSN: 0032-3861

Kim, N.-K.; Murall, A. & DeRose, V. J. (2004). A distance ruler for RNA using EPR and site-directed spin labeling. Chemistry & Biology, Vol. 11, No. 7, 939-948, *ISSN*: 1074-5521

Kokorin, A. I. (1974). *The measurement of distances between spin labels as a method of studying the structure of macromolecules and solid solutions*. Ph.D. Thesis, ICP AN SSSR, Moscow

Kokorin, A. I. (1986). Application of nitroxyle biradicals in medical-biological studies. In: *Method of Spin Labels and Probes. Problems and Perspectives*, N. M. Emanuel & R. I. Zhdanov (Eds.), 61-79, Nauka, Moscow

Kokorin, A. I. (1992). *The structure of coordination compounds with macromolecular ligands*. Dr.Sci. Thesis, ICP RAS, Moscow

Kokorin, A. I. & Formazyuk, V. E. (1981). New method of measuring distances between spin-label and paramagnetic ions in macromolecules. *Russ. Molek. Biol.*, Vol. 15, No. 4, 930-938 (p. 722-728 in transl.) ISSN 0026-8984

Kokorin, A. I. & Zamaraev, K. I. (1972). Investigation of the structure of frozen two-component solutions with the aid of iminoxy-radicals. *Russian J. Phys. Chem.*, Vol. 46, No. 11, 1658-1659, ISSN 0044-4537

Kokorin, A. I.; Kirsh, Yu. E. & Zamaraev, K. I. Determining local concentrations of units in macromolecular coils using the spin-labelling method. (1975). *Vysokomol. Soed.*, Vol. a17, No. 7, 1618-1621, (p. 1864-1868 in transl.) ISSN: 0507-5475

Kokorin, A. I.; Parmon, V. N. & Shubin, A. A. (1984). *Atlas of the anisotropic EPR spectra of nitroxide biradicals*. Nauka, Moscow

Kokorin, A. I.; Bogach, L. S.; Shapiro, A. B. & Rozantsev, E. G. (1976). Study of conformational peculiarities of triazine nitroxide biradicals by EPR technique. *Bull. Acad. Sci. USSR, Chemistry*, No. 9, 1994-1999, ISSN 0002 3353

Kokorin, A. I.; Molochnikov, L. S.; Yakovleva, I. V.; Shapiro, A. B. & Gembitskii, P. A. (1989). Study of the interaction of transition metal ions with polyethyleneimine using the spil-label method. *Vysokomol. Soed. A*, Vol. 31, No. 3, 546-551, ISSN: 0507-5475 (Russ. Ed.); *Polymer Sci. USSR* (1990), Vol. 31, No. 3, 597-603, ISSN: 0507-5475 (Engl. Ed.)

Kokorin, A. I.; Parmon, V. N.; Suskina, V. I.; Ivanov, Yu. A.; Rozantsev, E. G. & Zamaraev, K. I. (1974). Intramolecular exchange and dipole-dipole interactions in solutions of some iminoxyl biradicals. *Russ. J. Phys. Chem.*, Vol. 48, No. 4, 548-551, ISSN 0036-0244

Kokorin, A. I.; Zamaraev, K. I.; Grigoryan, G. L.; Ivanov, V. P. & Rozantsev, E. G. (1972). Measurement of the distances between the paramagnetic centres in solid solutions of nitroxide radicals, biradicals and spin-labeled proteins. *Biofizika*, Vol. 17, No. 1, 34-41 (p. 31-39 in transl.). ISSN 0006-3029

Kolbanovsky, A. D.; Wasserman A. M.; Kokorin, A. I. & Khazanovich, T. N. (1992a). Experimental verification of the theory of the dipole-dipole broadening of the EPR spectra of solid solutions of radicals. *Russ. J. Chem. Phys.*, Vol. 11, No. 1, 94-98, ISSN 0207-401X

Kolbanovsky, A. D.; Wasserman A. M.; Medvedeva, T. V. & Khazanovich, T. N. (1992b). EPR as a method for the determination of the spin-labeled macromolecule conformation in a solid state. *Russ. J. Chem. Phys.*, Vol. 11, No. 8, 1129-1135, ISSN 0207-401X

Kovarski, A. L. (1996). Spin probes and labels. A quarter of a century of application to polymer studies, in: *Polymer Yearbook*, R. A. Pethrick, Ed. Vol. 13, 113-139, ISBN 3-7186-5712-0

Kozlov, S. V.; Kokorin, A. I.; Shapiro, A. B. & Rozantsev, E. G. (1981). Chain nitroxide biradicals – a model for investigation the oligomers in solutions. *Vysokomolec. Soed. B*, Vol. 23, No. 5, 323-327, ISSN 0507-5475

Köhler, S. D.; Spitzbarth, M.; Diederichs, K.; Exner, T. E. & Drescher, M. (2011). A short note on the analysis of distance measurements by electron paramagnetic resonance. *J. Magn. Reson.*, Vol. 208, No. 1, 167–170, ISSN 1090-7807

Kruk, D.; Kowalewski, J.; Tipikin, D. S.; Freed, J. H.; Mo´scicki, M.; Mielczarek, A. & Port, M. (2011). Joint analysis of ESR lineshapes and ^{1}H NMRD profiles of DOTA-Gd derivatives by means of the slow motion theory. *J. Chem. Phys.*, Vol. 134(2), 024508, ISSN 0021-9606

Kulikov, A. V. (1976). Evaluation of the distance between spins of the spin label and paramagnetic centre in spin-labeled proteins from the parameters of saturation curve of EPR spectra of labels at 77 K. *Russ. Molek. Biol.*, Vol. 10, No. 1, 132-141, ISSN: 0026-8984

Kulikov, A. V. & Likhtenstein, G. I. (1974). The use of the saturation curves for estimation of distances in biological systems by the method of double spin labels. *Biofizika*, Vol. 19, No. , 420-423, ISSN 0006-3029

Kulikov, A. V. & Likhtenstein, G. I. (1977). The use of spin relaxation phenomena in the investigation of the structure of model and biological systems by the method of spin labels. *Adv. in Molec. Relax. and Interaction Processes*. Vol. 10, No. 1, 47-79, ISSN 0378-4487

Kulikov, A. V.; Likhtenstein, G. I.; Rozantsev, E. G.; Suskina, V. I. & Shapiro, A. B. (1972). On possible determination of distances between functional groups of protein by the method of spin labels. *Biofizika*, Vol. 17, No. 1, 42-48, ISSN 0006-3029

Kuznetsov, A. N. (1976). *The Method of Spin Probes*, Nauka, Moscow

Lagerstedt, J. O.; Budamagunta, M. S.; Oda, M. N. & Voss, J. C. (2007). EPR spectroscopy of site-directed spin labels reveals the structural heterogeneity in the N-terminal domain of ApoA-I in solution. *J. Biol. Chem.*, Vol. 282, No. 12, 9143–9149, ISSN 0021-. 9258

Lebedev, Ya. S. (1969). *Free radicals in the Solid State*, Dr. Sci. Thesis, ICP AN USSR, Moscow

Lebedev, Ya. S. & Muromtsev, V. I. (1971). *EPR and relaxation of the stabilized radicals*, Khimiya, Moscow

Leigh, J. S. (1970). ESR rigid-lattice line shape in a system of two interacting spins. *J. Chem. Phys.*, Vol. 52, No. 5, 2608-2612, ISSN 0021-9606

Likhtenshtein, G. I. (1974). *The Method of Spin Labels in Molecular Biology*, Nauka, Moscow; (1976). *Spin Labeling Methods in Moleculat Biology*. Wiley, *ISBN*-10: 0-4702-5882-9 New York

Likhtenshtein, G.; Yamauchi, J.; Nakatsuji, S.; Smirnov, A. I. & Tamura, R. (2008). *Nitroxides*: Applications in Chemistry, Biomedicine, a*nd Materials Science*, Wiley-VCH, ISBN: 978-3-527-31889-6, New York

Maksina, A. G.; Azizova, O. A.; Artemova, L. G.; Vladimirov, Yu. A. & Kokorin, A. I. (1979). Study of the location of spin-labeled thiol groups relatively the active center of Ca-depending ATP-ase. *Proc. Acad. Sci. USSR*, Vol. 247, No. 4, 982-985, ISSN 0891-5571

Mevorat-Kaplan, K.; Weiner, L. & Sheves, M. (2006). Spin labeling of *Natronomonas pharaonis* halorhodopsin: Probing the cysteine residues environment. *J. Phys. Chem. B*, Vol. 110, No. 17, 8825-8831, ISSN 1089-5647

Mikhalev, O. I.; Yakovleva, I. V.; Trofimov, V. J. & Shapiro, A. B. (1985). The ESR study of the structure of frozen aqueous solutions of Polyvinylpyrrolidone and Polyvinylalcohol. *Cryo-Letters*, No. 6, 245-256, ISSN 0143-2044

Misra, S. K., Ed. (2011). *Multifrequency Electron Paramagnetic Resonance: Theory and Applications*, Wiley-VCH, ISBN 978-3527407798,

Molin, Yu. N.; Salikov, K. M. & Zamaraev, K. I. (1980). *Spin Exchange*, Springer-Verlag, ISBN 3-540-10095-4, Berlin, New York

Möbius, K. & Savitsky, A. (2009). *High-field EPR Spectroscopy on Proteins and their Model Systems*, RSC Publishing, ISBN: 0-8540-4368-3

Neiman, M. B.; Rozantsev, E. G. & Mamedova, Yu. G. (1962). Free radical reactions involving no unpaired electrons. *Nature*, Vol. 196, 472-474, ISSN 0028-0836

Parmon, V. N. & Kokorin, A. I. (1976), unpublished results.

Parmon, V. N.; Kokorin, A. I. & Zhidomirov, G. M. (1977a). The interpretation of the polycrystalline ESR spectra of nitroxide biradicals. *J. Magn. Res.*, Vol. 28, No. 2, 339-349, ISSN 1090-7807

Parmon, V. N.; Kokorin, A. I. & Zhidomirov, G. M. (1977b). Conformational structure of nitroxide biradicals. Use of biradicals as spin probes. *Russ. J. Struct. Chem.*, Vol. 18, No. 1, 104-147, ISSN 0022-4766

Parmon, V. N.; Kokorin, A. I. & Zhidomirov, G. M. (1980). *Stable Biradicals*. Nauka, Moscow

Persson, M.; Harbridge, J. R.; Hammarström, P.; Mitri, R.; Mårtensson, L.-G.; Carlsson, U.; Eaton, G. R. & Eaton, S. S. (2001). Comparison of EPR methods to determine distances between spin labels on Human Carbonic Anhydrase II. *Biophys. J.*, Vol. 80, No. 6, 2886–2897, ISSN 0006-3495

Pittenger, J. T.; Hess, J. F.; Budamagunta, M. S.; Voss, J. C. & FitzGerald, P. G. (2008). Identification of phosphorylation-induced changes in Vimentin intermediate filaments by site-directed spin labeling and EPR. *Biochemistry*, Vol. 47, No. 41, 10863–10870, ISSN 0001527X

Popp, S.; Packschies, L.; Radzwill, N.; Vogel, K. P.; Steinhoff, H.-J. & Reinstein, J. (2005). Structural dynamics of the DnaK–peptide complex. *J. Mol. Biol.*, Vol. 347, No. 4, 1039–1052, ISSN 0022-2836

Pryce, M.H.L. & *Stevens*, K.W.H. (*1950*). The Theory of magnetic resonance-line widths in crystals. Proc. Phys. Soc. (London), Vol. A63, No. 1, 36-, ISSN 0370-1301

Rabenstein, M. D. & Shin, Y.-K. (1995). Determination of the distance between two spin labels attached to a macromolecule. *Proc. Nat. Acad. Sci. USA*, Vol. 92, No. , 8239-8243, ISSN 0027-8424

Reginsson, G. W. & Schiemann, O. (2011). Pulsed electron–electron double resonance: beyond nanometre distance measurements on biomacromolecules. *Biochem. J.*, Vol. 434, No. 2, 353–363, ISSN 0264-6021

Rozantsev, E. G. (1964). On free organic radicals with a hydroxy group. Izv. AN SSSR, Ser. Khim., No. 12, 2187-2191, *ISSN* 0002 3353

Rozantsev, E. G. (1970). *Free Iminoxyl Radicals*, Khimiya, Moscow. *Free Nitroxyl Radicals*, Plenum Press, *ISBN* 0-608-05755-X, New York

Rozantzev, E. G. & Neiman, M. B. (1964). Organic radical reactions involving no free valence. *Tetrahedron*, Vol. 20, No. 1, 131-137, ISSN: 00404020

Salikhov, K. M. (2010). Contributions of exchange and dipole–dipole interactions to the shape of EPR spectra of free radicals in diluted solutions. *Appl. Magn. Reson.*, Vol. 38, No. 2, 237-256, ISSN 0937-9347

Savitsky, A.; Dubinskii, A. A.; Zimmermann, H.; Lubitz, W. & M€obius, K. (2011). High-field dipolar EPR spectroscopy of nitroxide biradicals for determining three-dimensional structures of biomacromolecules in disordered solids. *J. Phys. Chem. B*, Vol. 115, No. 41, 11950-11963, ISSN 1089-5647

Saxena, S. & Freed, J. H. (1997). Theory of Double Quantum Two-Dimensional ESR with Application to Distance Measurements. *J. Chem. Phys.*, Vol. 107, No. 5, 1317–1340, *ISSN* 0021-9606

Schiemann, O.; Piton, N.; Plackmeyer, J.; Bode, B. E.; Prisner, T. F. & Engels, J. W. (2007). Spin labeling of oligonucleotides with the nitroxide TPA and use of PELDOR, a pulse EPR method, to measure intramolecular distances. *Nature Protocols, No.* 2, 904 – 923, ISSN 1754-2189

Schlick, S., Ed. (2006). *Advanced ESR Methods in Polymer Research*. Wiley, ISBN: 0-471-73189-7, Hoboken

Schweiger, A. & Jeschke, G. (2001). *Principles of Pulse Electron Paramagnetic Resonance*, Oxford University Press, *ISBN* 13: 978-0-19-850634-8, Oxford

Sergeev, P. V.; Ul'yankina, T. I.; Seifulla, R. D.; Grebenshchikov Yu. B. & Likhtenstein, G. I. (1974). Study of the interaction of steroids with human serum albumin by the spin label method. *Molec. Biol.*, Vol. 8, No. 2, 206-217, ISSN 0026-8984

Shaulov, A. Yu.; Kharitonov, A. S. & Kokorin, A. I. (1977). Analysis of the conformational state of the macromolecules in dilute and concentrated polymer solutions using spin labelling. *Polymer Sci. USSR*, Vol. 19, No. 8, 2075-2085, ISSN: 0507-5475

Steinhoff, H.-J. (2002). Methods for study of protein dynamics and protein-protein interaction in protein-ubiquitination by EPR spectroscopy. Frontiers in Bioscience, Vol. 7, c97-110, *ISSN* 1093-9946

Steinhoff, H.-J. (2004), Inter- and intra-molecular distances determined by EPR spectroscopy and site-directed spin labeling reveal protein-protein and protein-oligonucleotide interaction. *J. Biol. Chem.*, Vol. 385, No. 10, 913-920, ISSN 1431-6730

Steinhoff, H. J.; Radzwill, N.; Thevis, W.; Lenz, V.; Brandenburg, D.; Antson, A.; Dodson, G. & Wollmer, A. (1997). Determination of interspin distances between spin labels attached to insulin: comparison of EPR data with the X-ray structure. *Biophys. J.*, Vol. 73, No. 6, 3287-3298, ISSN 0006-3495

Tanford, C. (1961). *Physical Chemistry of Macromolecules*. Wiley, ISBN 0-19-850466-7, New York

Tsvetkov, Yu. D.; Milov, A. D. & Mar'yasov, A. G. (2008), Pulse electron-electron double resonance (PELDOR) as nanometre range EPR spectroscopy. *Usp. Khimii*, Vol. 77, No. 6 515-550 ISSN 0042-1308

Van Vleck, J. H. (1948). The dipolar broadening of magnetic resonance lines in crystals. *Phys. Rev.*, Vol. 74, No. ,1168-1183

Wasserman, A. M. & Kovarsky, A. L. (1986). *Spin Labels and Probes in Physical Chemistry of Polymers*, Nauka, Moscow

Wasserman, A. M.; Aleksandrova, T. A. & Kirsh, Yu. E. (1980a). The study of intramolecular mobility and of local density of poly-4-vinylpyridine units in solution with spin label method. *Vysokomolec. Soed. A*, Vol. 22, No. 2, 275-281, ISSN: 0507-5475

Wasserman, A. M.; Aleksandrova, T. A. & Kirsh, Yu. E. (1980b). The study of of local units density and of molecular dynamics in concentrated poly-4-vinylpyridine solutions with spin label method. *Vysokomolec. Soed. A*, Vol. 22, No. 2, 282-291, ISSN: 0507-5475

Wasserman, A. M.; Khazanovich, T. N. & Kasaikin, V. A. (1996). Some EPR spin probe and spin label studies of polymer systems. *Appl*. Magn. *Reson.*, Vol. 10, No. 1-3, 413-429, ISSN 0937-9347

Wasserman, A. M.; Aleksandrova, T. A.; Kirsch, Yu. E. & Buchachenko, A. L. (1979). Investigation of local density of monomer units and molecular dynamics in solutions of poly-4-vinyl-pyridine by the spin label technique. *Eur. Polymer J.*, Vol. 15, No. 11, 1051–1057, ISSN: 0014-3057

Wasserman, A. M.; Kolbanovsky, A. D.; Kokorin, A. I.; Medvedeva, T. V. & Khazanovich, T. N. (1992). Assessing the conformations of spin-labeled macromolecules in solid amorphous polymers using ESR. *Polymer SScience*, Vol. 34, No. 10, 858-862, ISSN: 0507-5475

Webb, G. A., Ed. (2006). *Modern Magnetic Resonance: I. Applications in Chemistry; II. Applications in Biological, Medical and Pharmaceutical Sciences Volume; III. Applications in Materials, Food and Marine Sciences*, Springer Verlag, ISBN 1-402-03894-1

Weil, J. A. & Bolton, J. R. (2007). *Electron Paramagnetic Resonance: Elementary Theory and Practical Applications*. Wiley & Sons, Inc., ISBN 978-0471754961, Hoboken

Weiner, L.; Shin, I.; Shimon, L. J. W. ; Miron, T.; Wilchek, M.; Mirelman, D.; Frolow, F. & Rabinkov, A. (2009). Thiol-disulfide organization in alliin lyase (alliinase) from garlic (*Allium sativum*). *Protein Sci.*, Vol. 18, No. 1, 196-205, ISSN 0961-8368

Zavriev, S. K.; Grigoryan, G. L. & Minchenkova, L. E. (1976). The study of DNA-Dye interaction by the method of spin labels. *Russ. Molek. Biol.*, Vol. 10, No. 5, 1387-1393, ISSN: 0026-8984

IntechOpen